


Spring 2012

# Smart Sensing and Performance Analysis for Cognitive Radio Networks

Yanxiao Zhao  
*Old Dominion University*

Follow this and additional works at: [https://digitalcommons.odu.edu/ece\\_etds](https://digitalcommons.odu.edu/ece_etds)

 Part of the [Computer Engineering Commons](#), and the [Electrical and Computer Engineering Commons](#)

---

## Recommended Citation

Zhao, Yanxiao. "Smart Sensing and Performance Analysis for Cognitive Radio Networks" (2012). Doctor of Philosophy (PhD), dissertation, Electrical/Computer Engineering, Old Dominion University, DOI: 10.25777/cfm4-bx62  
[https://digitalcommons.odu.edu/ece\\_etds/151](https://digitalcommons.odu.edu/ece_etds/151)

This Dissertation is brought to you for free and open access by the Electrical & Computer Engineering at ODU Digital Commons. It has been accepted for inclusion in Electrical & Computer Engineering Theses & Dissertations by an authorized administrator of ODU Digital Commons. For more information, please contact [digitalcommons@odu.edu](mailto:digitalcommons@odu.edu).

**SMART SENSING AND PERFORMANCE ANALYSIS FOR  
COGNITIVE RADIO NETWORKS**

by

Yanxiao Zhao

B.S. July 2001, Xi'an University of Architecture and Technology, China

M.S. March 2005, Xi'an Jiaotong University, China

A Dissertation Submitted to the Faculty of  
Old Dominion University in Partial Fulfillment of the  
Requirements for the Degree of


DOCTOR OF PHILOSOPHY

ELECTRICAL AND COMPUTER ENGINEERING

OLD DOMINION UNIVERSITY

May 2012

Approved by:

  
Min Song (Director)

  
Chunsheng Xin (Member)

  
Dimitrie C. Popescu (Member)

  
Linda L. Vahala (Member)

## **ABSTRACT**

# **SMART SENSING AND PERFORMANCE ANALYSIS FOR COGNITIVE RADIO NETWORKS**

Yanxiao Zhao

Old Dominion University, 2012

Director: Dr. Min Song

Static spectrum access policy has resulted in spectrum scarcity as well as low spectrum utility in today's wireless communications. To utilize the limited spectrum more efficiently, cognitive radio networks have been considered a promising paradigm for future network. Due to the unique features of cognitive radio technology, cognitive radio networks not only raise new challenges, but also bring several fundamental problems back to the focus of researchers. So far, a number of problems in cognitive radio networks have remained unsolved over the past decade. The work presented in this dissertation attempts to fill some of the gaps in the research area of cognitive radio networks. It focuses primarily on spectrum sensing and performance analysis in two architectures: a single cognitive radio network and multiple co-existing cognitive radio networks. Firstly, a single cognitive radio network with one primary user is considered. A weighted cooperative spectrum sensing framework is designed, to increase the spectrum sensing accuracy. After studying the architecture of a single cognitive radio network, attention is shifted to co-existing multiple cognitive radio networks. The weakness of the conventional two-state sensing model is pointed out in this architecture. To solve the problem, a smart sensing model which consists of three states is designed. Accordingly, a method for a two-stage detection procedure is developed to accurately detect each state of the three. In the first stage, energy detection is employed to identify whether a channel is idle or occupied. If the channel is occupied, received signal is further analyzed at the second stage to determine whether the signal originates from a primary user or an secondary user. For the second stage, a statistical model is developed, which is used for distance estimation. The false alarm and miss detection probabilities for the spectrum sensing technology are theoretically analyzed. Then, how to use smart sensing, coupled with a designed media access control protocol, to achieve fairness among multiple CRNs is thoroughly investigated. The media access control protocol fully takes the PU activity into account. Afterwards, the significant performance metrics including throughput and fairness are carefully studied. In terms of fairness, the fairness dynamics from a micro-level to macro-level is evaluated among secondary users from multiple cognitive

radio networks. The fundamental distinctions between the two-state model and the three-state sensing model are also addressed. Lastly, the delay performance of a cognitive radio network supporting heterogeneous traffic is examined. Various delay requirements over the packets from secondary users are fully considered. Specifically, the packets from secondary users are classified into either delay-sensitive packets or delay-insensitive packets. Moreover, a novel relative priority strategy is designed between these two types of traffic by proposing a “transmission window” strategy. The delay performance of both a single-primary user scenario and a multiple-primary user scenario is thoroughly investigated by employing queueing theory.

This work is in memory of my grandma, Shuran,  
dedicated to my parents, Zhiyong and Juncai,  
my husband, Hong,  
and my daughter, Katherine.

## ACKNOWLEDGEMENTS

Though this dissertation is an individual work, I would never have been able to finish it without the guidance, support and help from numerous people.

Firstly, I would like to express my deepest gratitude to my advisor, Dr. Min Song, for his excellent guidance, unfailing support, huge understanding and patience during my Ph.D. study. With his professional helps, I learned how to do research in a thorough and productive way. In addition, he sets a great career example for me in terms of his hard work, persistence and strong sense of responsibility.

I would like to deeply thank my co-advisor, Dr. Chunsheng Xin, who provides me countless technical discussions and valuable suggestions on my research. I am often inspired by his in-depth comments. I also learned much from his breadth of knowledge and modest manner as an outstanding researcher.

I would like to thank Dr. Dimitrie C. Popescu and Dr. Linda L. Vahala for serving as my committee members and constantly guiding my research for the past several years.

I would like to thank all the current and previous members in the Wireless Networking Lab. Without the stimulating discussions with them and their friendship, it would be a boring and lonely lab. Special thanks to Dr. Manish Wadhwa, Dr. Jun Wang, Jonathan Backens, Changlong Chen, Dr. Sachin Shetty, Gayathri Shivaraj, etc.

I would like to thank all my friends in Norfolk and in China. They are willing to give me a hand when I need helps and share wonderful moments with me as well. Many thanks to Yanhong Zhao, Rui Wang, Hui Sun, Bo Jiang, Xiaoyan Sun, Changlong Zhu, Jean, Li Fang, Lili Cao, Jing Chen, Xiaohui Liu, etc.

I would like to thank the Department of Electrical and Computer Engineering and the Old Dominion University Research Foundation for the financial support during my Ph.D. study.

I would like to thank my grandma with whom I grew up. She dedicated her whole life to her children and grandchildren, including me. I would like to thank my parents, parents-in-law, my aunt and my older brother. They are always supportive and encouraging during the pursuit of my personal and career goals.

Last, but not least, I would like to thank my husband, Hong, for his unconditional love, patience and support during my Ph.D. study. My precious daughter, Katherine, deserves my sincere gratitude as well. She never fails to cheer me up and make me happy with her charming smiles and laughter.

## TABLE OF CONTENTS

	Page
LIST OF TABLES . . . . .	ix
LIST OF FIGURES . . . . .	xi
<b>CHAPTER</b>	
<b>I INTRODUCTION . . . . .</b>	<b>1</b>
I.1 PROBLEM STATEMENT . . . . .	2
I.2 DISSERTATION CONTRIBUTIONS . . . . .	3
I.3 DISSERTATION OUTLINE . . . . .	6
<b>II BACKGROUND AND RELATED WORK . . . . .</b>	<b>7</b>
II.1 LOCAL SENSING . . . . .	7
II.2 COOPERATIVE SENSING . . . . .	9
II.3 MAC DESIGN IN CRNS . . . . .	11
II.4 PERFORMANCE ANALYSIS IN CRNS . . . . .	12
<b>III WEIGHTED COOPERATION SPECTRUM SENSING . . . . .</b>	<b>15</b>
III.1 SYSTEM MODEL AND MAIN IDEA . . . . .	16
III.2 ANALYSIS . . . . .	19
III.2.1 LOCAL SPECTRUM SENSING . . . . .	19
III.2.2 OPTIMAL DECISION MAKING AT THE BS . . . . .	21
III.2.3 MINIMUM NUMBER OF SUs REQUIRED FOR COOPERATIVE SENSING . . . . .	24
III.3 NUMERICAL RESULTS . . . . .	26
III.4 SUMMARY . . . . .	29
<b>IV SENSING TECHNOLOGY FOR THREE-STATE SENSING MODEL . . . . .</b>	<b>34</b>
IV.1 THREE-STATE SENSING MODEL AND METHODOLOGY . . . . .	36
IV.1.1 THREE-STATE SENSING MODEL . . . . .	36
IV.1.2 METHODOLOGY:TWO-STATE DETECTION PROCEDURE . . . . .	38
IV.2 IMPLEMENTATION OF TWO-STATE DETECTION . . . . .	38
IV.2.1 STATISTICAL MODEL FOR PROPAGATION DISTANCE . . . . .	39
IV.2.2 LOCAL SPECTRUM SENSING BASED ON DISTANCE ESTIMATION . . . . .	41
IV.2.3 COOPERATIVE SPECTRUM SENSING AMONG SUS . . . . .	45
IV.3 NUMERICAL RESULTS . . . . .	48
IV.3.1 LOCAL SPECTRUM SENSING SCENARIO . . . . .	48
IV.3.2 COOPERATIVE SPECTRUM SENSING SCENARIO . . . . .	49
IV.4 SUMMARY . . . . .	50
<b>V USING SMART SENSING TO ACHIEVE FAIRNESS AMONG MULTI-CRNS . . . . .</b>	<b>52</b>
V.1 SMART SENSING MODEL . . . . .	53
V.2 FMAC: FAIRNESS-ACHIEVED MAC DESIGN . . . . .	55
V.3 PERFORMANCE ANALYSIS . . . . .	58
V.3.1 PU ACTIVITY ANALYSIS . . . . .	58
V.3.2 SU ACCESS PROBABILITY . . . . .	60

V.3.3	SU THROUGHPUT ANALYSIS . . . . .	63
V.3.4	FAIRNESS MEASUREMENT . . . . .	65
V.4	NUMERICAL RESULTS . . . . .	67
V.4.1	THROUGHPUT EVALUATION . . . . .	68
V.4.2	FAIRNESS EVALUATION . . . . .	69
V.5	SUMMARY . . . . .	70
VI	DELAY ANALYSIS FOR CRNS SUPPORTING HETEROGENEOUS TRAF- FIC . . . . .	73
VI.1	NETWORK MODEL . . . . .	74
VI.2	SINGLE-PU SCENARIO . . . . .	76
VI.2.1	TWO PRIORITY SCHEMES . . . . .	76
VI.2.2	DELAY ANALYSIS IN SINGLE-PU SCENARIO . . . . .	78
VI.3	MULTIPLE-PU SCENARIO . . . . .	82
VI.3.1	DYNAMIC CHANNEL SELECTION ALGORITHM . . . . .	82
VI.3.2	DELAY ANALYSIS IN MULTIPLE-PU SCENARIO . . . . .	84
VI.4	NUMERICAL RESULTS . . . . .	86
VI.4.1	SINGLE-PU SCENARIO . . . . .	86
VI.4.2	MULTIPLE-PU SCENARIO . . . . .	87
VI.5	SUMMARY . . . . .	91
VII	CONCLUSIONS AND FUTURE RESEARCH . . . . .	96
VII.1	CONCLUSIONS . . . . .	96
VII.2	FUTURE RESEARCH . . . . .	98
	BIBLIOGRAPHY . . . . .	99
	VITA . . . . .	108



**LIST OF TABLES**

Table	Page
1 The comparison of $\gamma$ and $P_e^i$ between theoretical and simulation (denoted as 'Sim') results in Fig. 2. . . . .	27
2 Parameters for the numerical experiment . . . . .	49
3 Major parameters for the numerical experiment . . . . .	67

## LIST OF FIGURES

Figure	Page
1	Weighted cooperative spectrum sensing framework . . . . . 17
2	$P_f, P_m$ and $P_e$ under the moderately noisy environment . . . . . 30
3	$P_f, P_m$ and $P_e$ under the heavily noisy environment . . . . . 31
4	Comparison of the total error probability . . . . . 32
5	The total error probability with different number of SUs. . . . . 32
6	The minimum number of SUs ( $m$ ) required to the maximum tolerable error probability ( $\epsilon$ ) . . . . . 33
7	Distance estimation with a single SU (represented by the solid star) . . . . . 43
8	Distance estimation with two SUs in (a): the solid stars represent SUs and the solid circle represents another possible single source, which is symmetric to the PU; and three SUs in (b): solid stars represent SUs and three of them can determine a specific transmitter without ambiguity. . . . . 46
9	The trade-off relationship between $P_f$ and $P_m$ . . . . . 49
10	Distribution of 1 PU, 2 BSs and 150 SUs in 2-D space. SUs are randomly distributed. . . . . 50
11	Miss detection probability and false alarm probability: $P_m$ and $P_f$ is obtained in one group; $Q_m$ and $Q_f$ is further obtained with three leader SU. . . 51
12	Illustration of fairness-achieved MAC (FMAC) design with the two-state model shown in (a) and the three-state sensing model shown in (b). . . . . 56
13	PU activity modeling . . . . . 59
14	(a) illustrates the transition probability among $W_c$ states from $[0, W_c-1]$ , in which for each state it is possible to conduct a renewal process; (b) shows an example of the renewal process at a specific state $k$ . Note that this renewal process applies to each state from $[0, W_c-1]$ . . . . . 62
15	Normalized throughput comparison between the two-state model and the three-state sensing model: $P_0 = 0.8$ . . . . . 69
16	Saturation throughput comparison between the two-state model and the three-state sensing model: $P_0 = 0.8$ . . . . . 70
17	The normalized throughput influenced by the PU activity . . . . . 71
18	Jain Index from $\Delta_1$ to $\Delta_{20}$ . . . . . 72
19	ALFA comparison for 5 and 10 SUs with the two-state and three-state models 72
20	Virtual queue model to process PU and SU packets . . . . . 75
21	Optional caption for list of figures . . . . . 78
22	Mean delays of PUPs, DSPs and DIPs in the single-PU scenario . . . . . 87
23	Mean delays as a function of $\lambda_0$ in the single-PU scenario . . . . . 88
24	Channel access probability for SU1 . . . . . 89
25	Channel access probability for SU2 . . . . . 90
26	Mean delays under LACS and RCS in the multiple-PU scenario, with 5 channels and 10 SUs . . . . . 91
27	Mean delays under LACS and RCS in the multiple-PU scenario, with 5 channels and 20 SUs. . . . . 94

28	Mean delays in the multiple-PU scenario, as a function of $\lambda_0^m$ , with 5 channels and 10 SUs . . . . .	95
29	Mean delays in the multiple-PU scenario, as a function of $\lambda_0^m$ , with 5 channels and 20 SUs . . . . .	95

# CHAPTER I

## INTRODUCTION

Today's wireless communications are governed by the *static spectrum access* (SSA) policy, in which fixed spectrum bands are assigned to licensed users for exclusive access [1]. With the rapid proliferation of various wireless services, however, SSA is exhausting the radio spectrum. This leaves little or no spectrum for future demands, a problem known as *spectrum scarcity*. On the other hand, a large number of licensed spectrum bands are considerably under-utilized in both time and spatial domains, a problem known as *low spectrum utilization* [2].

These issues have motivated the development of *cognitive radio networks* (CRNs), allowing *secondary users* (SUs) to dynamically detect idle licensed bands and temporarily access them. In other words, SUs are allowed to utilize an idle licensed spectrum band provided that they withdraw from the band when *primary users* (PUs) start using it.

CRNs have been considered as a new paradigm for future network architecture. Due to the unique features of cognitive radio technology, CRNs raise new challenges. Furthermore, with the emergence of cognitive radio technology, many fundamental problems that were well studied for traditional wireless networks are being revisited. Over the past decade, there have been considerable research efforts on CRNs, such as spectrum sensing and dynamic spectrum allocation [3–8], MAC protocol design [9, 10], capacity analysis [11, 12], etc. However, many problems in CRNs remained unsolved so far. The work presented in this dissertation attempts to fill some of the gaps. It consists of a weighted spectrum sensing technology in an infra-structured CRN; a design of a novel smart three-state sensing model

in co-existing multi-CRNs; a new sensing technology to implement the three-state sensing model; performance analysis of smart sensing and the delay investigation on SU packets supporting heterogenous traffic.

## **I.1 PROBLEM STATEMENT**

Spectrum sensing plays two critical roles in CRNs. First, before an SU transmits a packet, it needs to sense the spectrum environment to find an available spectrum band (a band without PU signals), which is referred as a *channel* hereafter. Second, during the SU packet transmission, the SU needs to continue sensing its channel to detect if a PU signal appears or not. If yes, the SU needs to vacate the channel immediately to avoid interferences to PUs.

Spectrum sensing is quite a challenging problem. This is because an SU cannot have a direct measurement of the channel between a PU receiver and a PU transmitter. In fact, an SU cannot even measure if a PU receiver exists, e.g., a TV terminal. How to sense channels effectively and accurately is an open research area. The work in this dissertation makes an effort to solve this problem.

Performance is a significant aspect of evaluating wireless networks. It is well known that throughput, fairness and delay are important performance metrics in traditional networks. However, their analysis is relatively new in CRNs and still in their infancy. This dissertation primarily focuses on the throughput and fairness in co-existing multiple CRNs and delay analysis in a single CRN.

The main goals of this dissertation are listed as follows:

- To develop a spectrum sensing technology with accurate sensing.

- To build a novel sensing model which is applicable to the scenario in which multiple CRNs co-exist in an area.
- To design a sensing method to enable the new sensing model practical.
- To analyze how to use a smart sensing model to achieve fairness among multiple CRNs.
- To analyze the queuing delay in a single CRN with one-PU and multiple-PU scenarios supporting heterogenous traffic.

## **I.2 DISSERTATION CONTRIBUTIONS**

This dissertation is comprised of four major contributions. **The first contribution** is that a weighted cooperative spectrum sensing framework for infrastructure-based cognitive radio networks is designed, to increase the spectrum sensing accuracy. The framework contains two modules. In the first module, each SU performs local spectrum sensing and computes the total error probability, which combines the false alarm probability and the miss detection probability. The total error probability and the energy signal from the PU are then sent to the base station. In the second module, the base station makes a final decision after combining the weighted energy signals from all SUs. The final decision is then broadcasted back to all SUs. To reduce the computation complexity and communication overhead, the base station also instructs the SUs that have large total error probabilities not to report their local sensing results. A theoretical model for the proposed framework is designed, in which the minimum number of SUs required to participate in cooperative sensing, subject to a given total error probability, is derived.

**The second contribution** is that the scenario with multiple co-existing CRNs is brought into focus. To our best knowledge, there has been very limited effort in this area. The majority of existing spectrum sensing algorithms aim to detect the existence of a signal on a channel, i.e., they classify the channel into *busy* or *idle*, referred to as a two-state model in this dissertation. Once a signal is detected, an SU is restrained from transmission on this channel. While this two-state model works properly when there is only one CRN, it significantly limits the potential and fairness of spectrum access when there are multiple CRNs co-existing in an area. This is because if an SU from one CRN is continuously accessing the spectrum, SUs from all other CRNs would detect the channel as busy and hence starve. To solve this problem, a smart sensing model, i.e., a three-state sensing model is built. This is known as the first idea in recent studies. Specifically, this model distinguishes the channel as *idle*, *occupied by a PU*, or *occupied by an SU*. To accurately detect each state of the three, a methodology of a two-stage detection procedure is presented. In the first stage, energy detection is employed to identify whether a channel is idle or occupied. If the channel is occupied, received signal is further analyzed at the second stage to determine whether the signal originates from a PU or an SU. At the second stage, a statistical model is developed, which is used for distance estimation. The false alarm and miss detection probabilities for the spectrum sensing technology are theoretically analyzed.

**The third contribution** lies in analyzing how to use the smart sensing model to achieve fairness among SUs from multiple CRNs. To make this analysis complete, a *fairness-achieved media access control* (FMAC) protocol is designed. Associated with FMAC, a novel Markov chain model is developed, which fully takes the PU activity into account.

Afterwards, the significant performance metrics including throughput and fairness are carefully studied. In terms of fairness, the fairness dynamics from a micro-level to macro-level is evaluated among SUs from multiple CRNs. The fundamental distinctions between the two-state model and the three-state sensing model are also addressed. As far as we know, the three-state sensing model coupled with the thorough theoretical analysis on performance is investigated for the first time.

**The fourth contribution** is that the delay performance of a CRN supporting heterogeneous traffic is analyzed, an area which has received little attention. In order to guarantee PUs licensed membership, packets from PUs are distinguished from SUs by employing an absolute priority scheme. Unlike most of the previous studies that assumed all SUs are of the same priority, priority differentiation for SU packets is taken into account in this dissertation. The packets from SUs are classified into either delay-sensitive packets or delay-insensitive packets. Moreover, a novel relative priority strategy is designed between these two types of traffic by proposing a “transmission window” strategy. The delay performance of one-PU scenario and multiple-PU scenario is thoroughly investigated employing queuing theory. In the multiple-PU scenario, a dynamic and adaptive channel selection scheme based on learning automata is developed with the objective of reducing the average delay for all SU packets.



### **I.3 DISSERTATION OUTLINE**

The remaining part of this dissertation is organized as follows: Chapter II reviews the recent literature on CRNs that are related to this dissertation. In Chapter III, a weighted cooperative spectrum sensing framework for an infrastructure-based CRN is presented. Chapter IV firstly brings up a scenario in which multiple CRNs co-exist in an area and further points out the disadvantage of the conventional two-state sensing model. Afterwards, a smart three-state sensing model is designed to overcome this weakness. Specifically, the smart sensing is developed to achieve fairness among SUs from multiple CRNs. Furthermore, to enable this three-state sensing model's practical use, a methodology of a two-stage detection procedure, to accurately detect each of the three states, is presented. Chapter V is dedicated to analyzing the performance of the smart sensing model coupled with the proposed fairness-achieved MAC (FMAC). A Markov Chain is built to model it. Throughput and fairness is thoroughly analyzed based on the Markov chain model. Chapter VI focuses on the delay analysis for CRNs supporting heterogeneous traffic. Queueing delay is analyzed in both the single-PU and multiple-PUs scenarios. Conclusions and future research are summarized in Chapter VII.

## **CHAPTER II**

### **BACKGROUND AND RELATED WORK**

This chapter reviews the recent literature on spectrum sensing and performance analysis in CRNs. Due to the space limit, only the work closely related to this dissertation will be examined.

This chapter is organized as follows. The state-of-the-art technologies on spectrum sensing are first briefly introduced, including local sensing in Section II.1 and cooperative sensing in II.2. The related MAC design is summarized in II.3 and performance analysis is reviewed in II.4.

#### **II.1 LOCAL SENSING**

Spectrum sensing, that is, to detect the usage of channels, plays a critical role in CRNs. This is because SUs must be capable of sensing the spectrum environment accurately, and thus ensure that they will access the channel only when no PUs are present as well as withdraw immediately when PUs start using it. Spectrum sensing can be conducted via two modes: single-radio and dual-radio. In the former mode, the single radio is responsible for both spectrum sensing and data transmission. These two tasks are performed alternately. This mode is easy to implement and the cost is low. However, it is less efficient for the spectrum utilization. In the dual-radio mode, one radio keeps sensing all the time while the other one is dedicated for data transmission. This mode provides relatively high spectrum utilization with the cost of power consumption and implementation complexity.

Spectrum sensing in cognitive radio networks can be generally classified into two categories: local sensing and cooperative sensing. In local spectrum sensing, each SU independently makes a decision on channel availability based on the information collected. It will then attempt to access a selected channel if there are idle channels; otherwise, it keeps sensing.

A variety of individual sensing approaches have been proposed. Well-known techniques include matched filter detection, energy detection and cyclostationary feature detection. Theoretically, matched filter detection is the optimal solution for signal detection. Due to the considerable difficulty in implementation, however, this solution turns out to be more studied theoretically. Energy detection is a sub-optimal solution without any prior knowledge of the PU signal. It has low computation complexity and is easy to be implemented. However, it is susceptible to the uncertainty of noise power [13]. Furthermore, energy detection is not able to distinguish between noise and signal. To overcome the failure to differentiate signal from noise, cyclostationary feature detection attracts the focus of some researchers [14] [15]. Nevertheless, the computational complexity of this feature detection is significantly high.

All of three aforementioned approaches can be used alone, that is, with only one method involved during the spectrum sensing process. Another possible solution is to combine any two of them, which is referred to as two-stage spectrum sensing. A two-stage detection approach, combining energy detection and feature detection, was proposed in [16] [17]. The primary purpose of the existing two-stage detection method is to efficiently differentiate signal from noise. In addition to these three methods, several other approaches have been developed recently. Eigenvalue based method is designed in [18], which is based on the

eigenvalues of the covariance matrix of signals received at the SUs. As a powerful mathematical tool for analyzing signals, the wavelet based method is employed to detect the spectrum holes [19].

Location measurement is a potential solution to determine whether the signal is from a PU or not, given the location of PU is known. Location measurement has been studied in various fields, such as the security issue in wireless networks. The authors in [20] provide two methods to avoid malicious attacks against beacon-based location discovery in sensor networks. In [21], the authors present an attack-resilient cooperation stimulation system for autonomous ad hoc networks. The basic idea is to stimulate cooperation among selfish nodes and defend against malicious attacks. In this dissertation, a distance estimation, instead of location estimation, is employed. Specifically, the possible range of the transmitter location rather than a specific estimated location of the transmitter is estimated. In this way, the computational complexity will be remarkably reduced.

## **II.2 COOPERATIVE SENSING**

An individual SU is not sufficient to provide accurate detection results. This is because an SU may experience severe fading, shadowing and other issues in the complicated wireless environment. Consequently, cooperations among SUs are required to improve the detection accuracy, which is known as cooperative sensing.

In cooperative sensing, each SU independently performs local spectrum sensing and makes a binary decision (idle or occupied) for a channel. This channel is determined as idle by cooperative sensing if all SUs (or a certain number of SUs) find that it is idle. The reader is referred to [3] [22] for the benefits of cooperative sensing. Cooperative sensing

can be implemented in a centralized or a distributed mode. In the centralized mode (e.g., see [6]), a base station (BS) collects the local sensing information from all SUs, and then makes the final decision. In the distributed mode (e.g., see [4]), SUs exchange local sensing information with each other and vote for a final decision.

Many cooperative sensing schemes have been proposed recently. The detection accuracy and sensing efficiency have been studied in [23], where a theoretical framework was developed to optimize sensing parameters to maximize the sensing efficiency, subject to the interference avoidance constraint. In [24], a coalitional game strategy is proposed to analyze the behavior of SUs in distributed cooperative sensing. The relation of the detection accuracy and sensing efficiency was modeled as a non-transferable coalitional game. In [25], the authors proposed a technique that uses a varying number of samples, and introduced a reputation-based mechanism to the sequential probability ratio test. In [26], SUs are divided into a few groups and each group chooses a head with the highest *signal-to-noise ratio* (SNR). Each SU reports its local sensing result to its head which makes a preliminary decision based on the reports from its members. Afterwards, group heads report their decisions to the BS. The BS makes a final decision using an “OR” rule, i.e., the result is 1 (channel is occupied by PU) as long as one group head report is 1. In [5], a weighted cooperative sensing is proposed based on the SNR, with the objective to maximize the detection sensitivity while meeting a given requirement on the false alarm probability. An SU’s weight is decreased if it experiences a lower SNR. The authors in [27] propose another weighted cooperative sensing scheme, with the motivation of equal probabilities of false alarm and miss detection. The idea is that SUs with large SNR are assigned with large weights and thus yield more contributions to the global decision. However, as pointed out in [28], in

the presence of noise uncertainty, SUs below a certain SNR cannot improve their performance even with infinite sensing time. In other words, SNR is not a suitable parameter to be used for selecting weights, because of its uncertainty in noise power. In addition, it is well acknowledged that there is a trade-off between the false alarm probability and the miss detection probability. Thus, optimizing one of them as in [5], or simply constraining them to be equal and then optimizing one of them as in [27], does not fully consider this trade-off.

### **II.3 MAC DESIGN IN CRNS**

The birth of CRNs occurred over a decade ago, however, the MAC design in CRNs is still in its infancy. The IEEE 802.22 working group has been making efforts on proposing a standard MAC protocol. Currently, the group concentrates primarily on the TV frequency spectrum [29]. A general MAC design in CRNs is still an open question and has received more and more consideration recently.

In [30], the authors develop a decentralized cognitive MAC protocol in Ad Hoc Networks. The sensing errors and collisions between SUs and PUs are taken into account. In [9], a MAC protocol is designed for multi-channel wireless networks. Each available channel is divided into recurring superframes. To coordinate among SUs, a rendezvous channel is assigned delicately. Several researchers have dedicated themselves to designing a cognitive MAC based on the well-known IEEE 802.11. The authors in [31] consider a CRN with a single channel and assume the PU operates on a slot-by-slot basis. They further divide each slot into mini-slots for SUs' transmission. In [32], the authors design a periodic MAC protocol, in which SUs cooperate to periodically sense channels, report channel states and exchange control signals. The protocol is analyzed based on the

two-state model.

In all the above work on MAC, the two-state model is predominantly employed. Meanwhile, most existing MAC protocols target the throughput improvement while the fairness performance receives limited attention. In this dissertation, to fill the void, a MAC with a goal to achieve fairness among SUs from multi-CRNs is designed.

#### **II.4 PERFORMANCE ANALYSIS IN CRNS**

Performance analysis is a significant perspective in CRNs, whereas throughput has received considerable attention. The throughput limit in the presence of dynamic and distributed spectral activity is studied in [11]. *Quality of service* (QoS) has recently become involved in the throughput analysis. In [33], QoS provisioning for voice service is considered. In [34], the two-state sensing model is employed. Based on this model, the performance of SU transmission over time-selective flat fading channels is studied. The QoS constraints and channel uncertainty is taken into account.

Fairness is another important performance metric that started obtaining attention recently. The authors in [35] consider the fairness in scheduler design for distributed CRNs. A timer mechanism is developed to achieve round-robin, max-min and proportional fairness in a CRN. Proportional fairness of two SU groups in a cognitive radio (CR) network is studied in [36]. In contrast, the research on fairness of SUs among multiple CRNs is fairly few. In this dissertation, co-existing multiple CRNs is one of major concerns. Accordingly, a smart three-state model is developed to achieve fairness among multi-CRNs. To our best knowledge, it is the first time fairness performance among multiple CRNs has been evaluated.

Traffic delay is also a critical network performance metric. However, there have been few studies on traffic delay in CRNs. Queueing theory is utilized in [37] to analyze the stable throughput of cognitive radios with and without relaying. Specifically, the analysis included: 1) random packet arrivals; 2) sensing errors at the secondary link; and 3) power allocation at the secondary transmitter. However, the authors in [37] only consider a two single-link users model, one PU and one SU. In this dissertation, a model with multiple PUs and multiple SUs is studied, which is the common case for typical CRNs.

The authors in [38] also utilize queueing theory to derive bounds for the throughput and delay of SU traffic in CRNs. They consider a network model in which all PUs and SUs are in a single-hop single-channel network. Hence, the channel selection for SUs was ignored. Most studies on CRNs assume that the bandwidth of every channel is the same, and thus the data rate on different channels is the same from the point of view of SUs. The work in [39] considers heterogenous bandwidth of channels, but focuses on a CRN consisting of SUs only, without consideration for coexistence of PUs and SUs. The authors in [40] take the heterogenous multimedia users into account. All their work is based on an absolute priority scheme over SUs. In this dissertation, a more general network model is considered and hence is significantly more practical than the previous studies. The complicated coexistence of PUs and SUs are taken into consideration. Furthermore, a novel priority differentiation using relative priority strategy among SUs is proposed. Finally, delay analysis of PUPs, DSPs and DIPs is exploited, via coupling queueing theory and channel selection strategy.

In a multiple-channel CRN, one fundamental problem is how to select an appropriate channel for each SU. In this dissertation, *learning automata* (LA) is employed to design a novel channel selection algorithm, with the objective of reducing the average delay for SU



packets. LA was invented decades ago [41] and has evolved into a powerful tool to facilitate network design. For instance, in [42, 43], LA has been used to develop a stochastic channel selection scheme for CRNs, with the objective to maximize the probability of successful transmission.

## CHAPTER III

### WEIGHTED COOPERATION SPECTRUM SENSING

Spectrum sensing plays a critical role in cognitive radio networks. A good sensing scheme can reduce both the false alarm and the miss detection probabilities, and thus improves spectrum utilization. In this chapter, a new metric, *total error probability*, is proposed to measure the accuracy of spectrum sensing. A unique feature of the total error probability is that it combines both the false alarm probability and the miss detection probability, as well as takes the PU activity into account. A weighted cooperative spectrum sensing framework for infrastructure-based cognitive radio networks is designed. Two modules are included in the framework. In the first module, each SU performs local spectrum sensing and computes the total error probability. Instead of simply providing a binary decision, the total error probability and the energy signal from the PU are sent to the *base station* (BS). In the second module, the BS makes a final decision after combining the information from all SUs and notifies them with the final decision. To take the fading and shadowing into account, the sensing information from a SU that has a higher total error probability is assigned with a lower weight. To minimize the detection error probability, an optimal threshold is derived. For SUs that have large total error probabilities, their local sensing results have negligible contribution to the decision making at the BS. To reduce the computation complexity and communication overhead, it is not necessary for every SU to participate in cooperative sensing. The minimum number of SUs required to participate in cooperative sensing is also studied.

This chapter is organized as follows. Section III.1 introduces the network model and

the main idea. Section III.2 presents the detailed design of the proposed spectrum sensing framework along with in-depth analysis. The numerical results are presented in Section III.3. Summaries are concluded in Section III.4

### III.1 SYSTEM MODEL AND MAIN IDEA

An infrastructure-based cognitive radio network is considered, which consists of one PU, one BS, and  $M$  SUs. SUs opportunistically share a licensed channel with the PU for data transmission. From the perspective of SUs, the channel simply alternates between *idle* (no PU activity) and *occupied* (with PU activity) status. Note that the status of idle or occupied is observed at the session level, rather than at the packet transmission level. The short quiet intervals between packet transmissions should not be counted as ‘usable’ idle periods by a good channel selection algorithm in CRNs. The channel selection algorithms should select the channels that have been idling for the relatively long period of time which happens between two consecutive communication sessions. The channel idle/occupied durations are assumed as independent random variables, and the channel activity is modeled as a semi-Markov process. Let  $H_0$  and  $H_1$  denote the event that the channel is in idle or occupied status, respectively. Let  $\alpha$  and  $\beta$  denote the mean occupied and idle durations of the channel, respectively. Then, the probabilities of the channel being idle and occupied are given as:

$$P(H_0) = \frac{\beta}{\alpha + \beta}, P(H_1) = \frac{\alpha}{\alpha + \beta}. \quad (1)$$

SUs use energy detection for local spectrum sensing. The PU’s signal is assumed reasonably higher than the noise level. A basic hypothesis model for the local spectrum sensing can be defined as follows:

$$x_i = \begin{cases} n_i, & \text{if } H_0 \\ s + n_i, & \text{if } H_1 \end{cases} \quad (2)$$

where  $x_i$  is the signal that SU  $i$  received,  $n_i$  is the zero-mean additive white Gaussian noise (AWGN), i.e.,  $n_i \sim \mathcal{N}(0, \sigma_i^2)$ , and  $s$  is the signal that the PU transmits. The channel gain is ignored because it is often assumed to be constant during the detection interval.

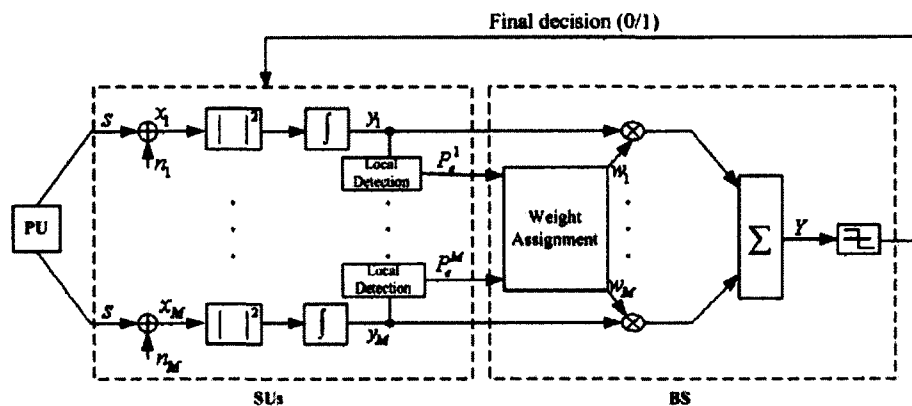


Fig. 1: Weighted cooperative spectrum sensing framework

The weighted cooperative sensing framework has two modules as shown in Fig. 1. In the first module, each SU performs local spectrum sensing and computes the total error probability. The total error probability and the energy signal are then sent to the BS through a common control channel. For the local sensing process of SU  $i$ , the received signal  $x_i$  is first pre-filtered by an ideal band-pass filter. The output of the band-pass filter is then squared and integrated over the observation period. The output of the  $i^{\text{th}}$  integrator representing the energy signal from the  $i^{\text{th}}$  SU, denoted by  $y_i$ , is compared with a local threshold  $\gamma^i$  to make a local sensing decision. The accuracy of the local sensing decision is characterized by a *total error probability*, defined as follows,

$$P_e^i = P(H_0) \cdot P_f^i + P(H_1) \cdot P_m^i \quad (3)$$

where  $P_f^i = P(y_i > \gamma^i | H_0)$  represents the false alarm probability, and  $P_m^i = P(y_i < \gamma^i | H_1)$  represents the miss detection probability. Notice that both  $P_m^i$  and  $P_f^i$  are conditional probabilities. Thus, the measurement of the total error probability takes the PU activity into account.

In the second module, the BS makes a final decision after combining the weighted energy signals and then notifies all SUs with the final sensing decision. To differentiate the local sensing accuracy, a SU that has a higher total error probability is assigned with a lower weight. Mathematically, the output from the BS can be written as:

$$Y = \sum_{i=1}^M w_i \cdot y_i, \quad i = 1, 2, \dots, M, \quad (4)$$

where  $w_i$  is the weight of the  $i^{\text{th}}$  SU. The output of the BS is then compared with a decision threshold  $\gamma$ . If  $Y \geq \gamma$ , the channel is determined to be occupied by the PU; otherwise, the channel is determined to be idle. This decision is then broadcasted to all SUs. Before presenting the details of each module in the next section, the performance of the generic cooperative spectrum sensing is first analyzed.

In the generic cooperative spectrum sensing (e.g., [44] [45]), a channel is determined to be idle only if all SUs report the channel idle status to the BS. As a result, the false alarm probability  $P_f$  and the miss detection probability  $P_m$  can be derived as follows:

$$P_f = 1 - \prod_{i=1}^M (1 - P_f^i), \quad (5)$$

$$P_m = \prod_{i=1}^M P_m^i. \quad (6)$$

Correspondingly, the total error probability  $P_e$  is:

$$\begin{aligned}
 P_e &= P(H_0) \cdot P_f + P(H_1) \cdot P_m \\
 &= \frac{\beta}{\alpha + \beta} \cdot \left[ 1 - \prod_{i=1}^M (1 - P_f^i) \right] + \frac{\alpha}{\alpha + \beta} \cdot \prod_{i=1}^M P_m^i.
 \end{aligned} \tag{7}$$

Since  $P_m^i$  is in the range  $(0, 1)$ ,  $P_m \ll P_m^i$ , which means that the generic cooperative sensing substantially decreases the miss detection probability. The price paid, however, is the considerable increment of false alarm probability, since  $P_f \gg P_f^i$ . As a result, the generic cooperative sensing does not perform well in terms of the total error probability (which will be verified in Section III.3).

## III.2 ANALYSIS

### III.2.1 LOCAL SPECTRUM SENSING

Let the bandwidth of the ideal band-pass filter be  $W$ . Then, the number of samples during the sensing period  $T$  is  $N = 2T \cdot W$ . Let  $N_0^i$  denote the two-sided noise power density spectrum at SU  $i$ . Then, the noise variance  $\sigma_i^2 = 2N_0^i \cdot W$ . The output of the  $i^{\text{th}}$  integrator with  $N$  samples can be represented as:

$$y_i = \sum_{k=1}^N |x_i(k)|^2, \quad i = 1, 2, \dots, M. \tag{8}$$

Here,  $y_i$  is the sum of the square of  $N$  independent Gaussian distributed random variables.

As such,  $y_i$  follows the chi-square distribution, i.e.,

$$\frac{y_i}{\sigma_i^2} \sim \begin{cases} \chi_N^2 & \text{if } H_0 \text{ (chi-square)} \\ \chi_N^2(\lambda_i) & \text{if } H_1 \text{ (noncentral chi-square)} \end{cases} \quad (9)$$

where  $\lambda_i = \frac{2E_s \cdot W}{\sigma_i^2}$ , and  $E_s$  is the signal energy [46].

According to the central limit theorem [47], the chi-square distribution approaches a normal distribution when the degree of freedom,  $N$ , increases. Specifically,

$$\frac{y_i}{\sigma_i^2} \sim \begin{cases} \mathcal{N}(N, 2N) & H_0 \\ \mathcal{N}(N + \lambda_i, 2(N + \lambda_i)) & H_1 \end{cases} \quad (10)$$

$$\Rightarrow y_i \sim \begin{cases} \mathcal{N}(N \cdot \sigma_i^2, 2N \cdot \sigma_i^4) & H_0 \\ \mathcal{N}((N + \lambda_i) \cdot \sigma_i^2, 2(N + 2\lambda_i) \cdot \sigma_i^4) & H_1 \end{cases} \quad (11)$$

The (conditional) means and variances of  $y_i$  are represented as:

$$E(y_i|H_0) = N \cdot \sigma_i^2 \quad (12)$$

$$\text{Var}(y_i|H_0) = 2N \cdot \sigma_i^4 \quad (13)$$

$$E(y_i|H_1) = (N + \lambda_i) \cdot \sigma_i^2 \quad (14)$$

$$\text{Var}(y_i|H_1) = 2(N + 2\lambda_i) \cdot \sigma_i^4 \quad (15)$$

As discussed in the last section, a threshold-based approach is used in cooperative sensing to determine the channel status. Specifically, for the  $i^{\text{th}}$  SU, if  $y_i$  is larger than a threshold  $\gamma^i$ , the channel is seen as occupied. The false alarm probability  $P_f^i$  and miss detection probability  $P_m^i$  can be calculated as:

$$P_f^i = Pr(y_i > \gamma^i | H_0) = Q\left(\frac{\gamma^i - E(y_i | H_0)}{\sqrt{Var(y_i | H_0)}}\right) \quad (16)$$

$$P_m^i = Pr(y_i \leq \gamma^i | H_1) = 1 - Q\left(\frac{\gamma^i - E(y_i | H_1)}{\sqrt{Var(y_i | H_1)}}\right) \quad (17)$$

where  $Q$  is the Q-function or tail probability of Gaussian distribution. Substituting Eqs. (16) and (17) into Eq. (3), it is straightforward to get the total error probability. The derivation of the optimal threshold  $\gamma^{i*}$  for the  $i^{th}$  SU, because it follows the same rationale as the derivation of the optimal threshold  $\gamma^*$  for the BS which will be described in the next subsection.

### III.2.2 OPTIMAL DECISION MAKING AT THE BS

Two issues need to be addressed for the BS to make a decision on the channel status. First, how to assign an appropriate weight to each SU in order to alleviate the fading and shadowing effects. Second, what is the optimal threshold to be used by the BS in order to minimize the total error probability?

The basic idea for weight assignment is that a SU with a higher error probability is assigned with a lower weight, as illustrated in **Algorithm 1**. First, the weight of each SU is computed based on the error probability. Then, all weights are normalized to satisfy  $\sum_{i=1}^M w_i(k) = 1$ .

With the assigned weight for each SU, the output signal at the BS is  $Y = \sum_{i=1}^M w_i y_i$ . Due to the fact that all  $y_i$  ( $1 \leq i \leq M$ ) are independent random variables following Gaussian distribution and  $w_i$  can be viewed as a constant in each sensing period,  $Y$  should also follow



---

**Algorithm 1** Weight Assignment
 

---

**Input:**  $P_e^i$  for  $(i = 1, \dots, M)$

- 1: **for**  $i = 1$  to  $M$  **do**
  - 2:    $w_i^* = 1/P_e^i$
  - 3: **end for**
  - 4: **for**  $i = 1$  to  $M$  **do**
  - 5:    $w_i = w_i^* / \sum_{k=1}^M w_k^*$
  - 6: **end for**
- 

a Gaussian distribution, i.e.,

$$Y \sim \begin{cases} \mathcal{N}(\sum_{i=1}^M w_i \cdot E(y_i|H_0), \sum_{i=1}^M w_i^2 \cdot \text{Var}(y_i|H_0)) & H_0 \\ \mathcal{N}(\sum_{i=1}^M w_i \cdot E(y_i|H_1), \sum_{i=1}^M w_i^2 \cdot \text{Var}(y_i|H_1)) & H_1 \end{cases} \quad (18)$$

The (conditional) means and variances of  $Y$  are denoted as:

$$E(Y|H_0) = \sum_{i=1}^M w_i \cdot E(y_i|H_0) \quad (19)$$

$$\text{Var}(Y|H_0) = \sum_{i=1}^M w_i^2 \cdot \text{Var}(y_i|H_0)$$

$$E(Y|H_1) = \sum_{i=1}^M w_i \cdot E(y_i|H_1) \quad (20)$$

$$\text{Var}(Y|H_1) = \sum_{i=1}^M w_i^2 \cdot \text{Var}(y_i|H_1) \quad (21)$$

Let  $\gamma$  denote the threshold to determine channel status by the BS, i.e., if  $Y > \gamma$ , then BS determines that the channel is occupied. Then the false alarm probability  $P_f$  and miss detection probability  $P_m$  of the weighted cooperative spectrum sensing can be derived as:

$$P_f = \Pr(Y > \gamma|H_0) = Q\left(\frac{\gamma - E(Y|H_0)}{\sqrt{\text{Var}(Y|H_0)}}\right),$$

$$P_m = \Pr(Y \leq \gamma|H_1) = 1 - Q\left(\frac{\gamma - E(Y|H_1)}{\sqrt{\text{Var}(Y|H_1)}}\right). \quad (22)$$

Accordingly, the total error probability  $P_e$  can be computed as:

$$\begin{aligned}
P_e &= P(H_0) \cdot P_f + P(H_1) \cdot P_m \\
&= \frac{\beta}{\alpha + \beta} \cdot Q\left(\frac{\gamma - E(Y|H_0)}{\sqrt{\text{Var}(Y|H_0)}}\right) + \\
&\quad \frac{\alpha}{\alpha + \beta} \cdot \left\{ 1 - Q\left(\frac{\gamma - E(Y|H_1)}{\sqrt{\text{Var}(Y|H_1)}}\right) \right\} \\
&= \frac{\beta}{\sqrt{2\pi} \cdot (\alpha + \beta)} \cdot \int_{\frac{\gamma - E(Y|H_0)}{\sqrt{\text{Var}(Y|H_0)}}}^{+\infty} e^{-\frac{t^2}{2}} dt + \\
&\quad \frac{\alpha}{\sqrt{2\pi} \cdot (\alpha + \beta)} \cdot \left( 1 - \int_{\frac{\gamma - E(Y|H_1)}{\sqrt{\text{Var}(Y|H_1)}}}^{+\infty} e^{-\frac{t^2}{2}} dt \right).
\end{aligned}$$

To minimize the total error probability  $P_e$ , its derivative is computed as:

$$\begin{aligned}
\frac{\partial(P_e)}{\partial(\gamma)} &= -\frac{\beta}{\sqrt{2\pi} \cdot (\alpha + \beta) \cdot \sqrt{\text{Var}(Y|H_0)}} \cdot e^{-\frac{1}{2} \left[ \frac{\gamma - E(Y|H_0)}{\sqrt{\text{Var}(Y|H_0)}} \right]^2} \\
&\quad + \frac{\alpha}{\sqrt{2\pi} \cdot (\alpha + \beta) \cdot \sqrt{\text{Var}(Y|H_1)}} \cdot e^{-\frac{1}{2} \left[ \frac{\gamma - E(Y|H_1)}{\sqrt{\text{Var}(Y|H_1)}} \right]^2}.
\end{aligned}$$

Let

$$\frac{\partial(P_e)}{\partial(\gamma)} = 0. \quad (23)$$

The optimal threshold  $\gamma^*$  to obtain the minimum total error probability ( $P_e$ ) is as follows

$$\gamma^* = \frac{E(Y|H_1)\text{Var}(Y|H_0) - E(Y|H_0)\text{Var}(Y|H_1) - \frac{1}{2}\sqrt{\Delta}}{[\text{Var}(Y|H_0) - \text{Var}(Y|H_1)]}, \quad (24)$$

where

$$\begin{aligned}
\Delta &= [2E(Y|H_0) \cdot \text{Var}(Y|H_1) - 2E(Y|H_1) \cdot \text{Var}(Y|H_0)]^2 \\
&\quad - 4[\text{Var}(Y|H_0) - \text{Var}(Y|H_1)] \cdot \left\{ \text{Var}(Y|H_0) \cdot E(Y|H_1)^2 \right. \\
&\quad \left. - \text{Var}(Y|H_1) \cdot E(Y|H_0)^2 + 2\text{Var}(Y|H_0) \cdot \text{Var}(Y|H_1) \cdot \right. \\
&\quad \left. \ln \left[ \frac{\beta \cdot \sqrt{\text{Var}(Y|H_1)}}{\alpha \cdot \sqrt{\text{Var}(Y|H_0)}} \right] \right\}.
\end{aligned} \quad (25)$$

The shape of  $P_e$  and the existence of the minimum of  $P_e$  are shown in Figs. 2 and 3 (to be discussed in Section III.3). With the optimal threshold  $\gamma^*$  available, the BS then compares its output  $Y$  with this threshold to determine if the channel is occupied (if  $Y > \gamma^*$ ). The BS then broadcasts this decision to all SUs. Note that Eq. (24) can also be used by each SU to calculate the optimal local threshold  $\gamma^{j*}$  by replacing  $Y$  with  $y_i$ .

### III.2.3 MINIMUM NUMBER OF SUs REQUIRED FOR COOPERATIVE SENSING

One way to reduce the computation complexity and communication overhead of the weighted cooperative spectrum sensing is to reduce the number of SUs involved in the decision-making. For SUs that have large total error probabilities and thus low weights, their local sensing results have negligible contribution to the decision making at the BS. As such, a sound decision can still be made at the BS even though these SUs do not participate in cooperative sensing. On the other hand, if these SUs do not need to participate, i.e., transmit their local sensing information to the BS, the computation complexity and communication overhead can be reduced, particularly in large networks.

Let  $\epsilon$  denote the maximum tolerable error probability, and  $m$  denote the minimum number of SUs required to participate in cooperating sensing, under the constraint that the total error probability is not larger than  $\epsilon$ . To find  $m$ , the BS first sorts all SUs by their weights at the descending order. Noticing that the total error probability  $P_e$  is a non-increasing function with respect to the number of SUs, the following equation holds

$$m = \arg \min_i \{P_e(i) \leq \epsilon\}, \quad (26)$$

where  $P_e(i)$  is the total error probability when the BS makes the decision based on the local sensing information of the first  $i$  SUs.

By the time the BS broadcasts its decision to all SUs, it will also announce the cut-off total error probability  $\zeta = P_e(m)$  (the total error probability of the  $m$ th SU in the sorted list). In the next sensing period, each SU will utilize the cut-off probability  $\zeta$  as a guide to determine if it needs to send its local sensing result to the BS. Specifically, after the SU performs the local spectrum sensing, if the computed total error probability is larger than  $\zeta$ , then this SU does not need to report the local sensing result to the BS. Thus, both the computation complexity at the BS and the communication overhead between SUs and the BS are reduced. One may note that  $\zeta$  has actually been determined based on the sensing results in the current sensing period, and may not be exactly the same as the one for the next sensing period. This issue can be resolved by two techniques. First, a margin can be added to the cut-off probability to accommodate the sensing variations in the next period, i.e., using a larger value than  $P_e^m$ , e.g., announcing  $\zeta = P_e^{m+j}$  ( $j > 0$ ) instead of  $\zeta = P_e^m$  (note that with the sorted list,  $P_e^{m+j} \geq P_e^m$ ) holds. Second, if in a sensing period, the total error probability  $P_e$  computed by the BS based on the sensing information of all reported SUs is larger than  $\epsilon$ , this means that the cut-off probability  $\zeta$ , announced in the last sensing period, was too small, and, based on the difference between  $\epsilon$  and  $P_e$ , a properly adjusted cut-off probability  $\zeta + \Delta$  will be announced for the next sensing period, so that more SUs will send their sensing results to the BS, to obtain a smaller  $P_e \leq \epsilon$ .

### III.3 NUMERICAL RESULTS

In this section, the performance of the proposed weighted cooperative spectrum sensing is evaluated. 10 SUs are considered unless otherwise noted. Without loss of generality, the transmitted PU signal is assumed to be  $s(k) = 1$ .

First, a *moderately noisy* environment is considered, where for each SU, the noise variances  $\sigma_i$  are randomly generated as Gaussian distribution with mean 0 and variance 1. Fig. 2 illustrates the false alarm probability  $P_f$ , the miss detection probability  $P_m$ , and the total error probability  $P_e$  as a function of the decision threshold  $\gamma$ , when  $P(H_0) = 0.2, 0.5$  and  $0.9$ , respectively.

It can be seen that in Fig. 2, the false alarm probability decreases when the threshold increases. This fits well with the physical meaning of the false alarm. That is, when the decision threshold is low, it is prone to incorrectly detect the presence of PU. With the threshold increasing, the false alarm probability decreases, and drops to a small value at the optimal threshold. The miss detection probability, however, increases along with the threshold. The figure also shows the inherent trade-off relationship between the false alarm probability and the miss detection probability. The total error probability also changes with varying thresholds. The minimum total error probability is obtained at the optimal threshold. Table 1 compares the theoretical results obtained by Eq. (24) and the simulation results with regard to the optimal threshold and the corresponding total error probability. Clearly they match very well. Note that the use of  $P_e$  as the performance metric is a good trade-off between the miss detection and the false alarm probabilities, although other combinations of miss detection and false alarm probabilities as performance metrics are also possible. This is because the minimum of  $P_e$  is usually obtained at a point where the miss detection

and false alarm probabilities are at the expected values for the corresponding user activity. For instance, the scenario with  $P(H_0) = 0.9$  and  $P(H_1) = 0.1$  is examined, which indicates that the PU has a low duty cycle. The system obtains the minimum  $P_e$  when  $P_f = 0.05$  and  $P_m = 0.34$ , i.e., the false alarm probability is low and the miss detection probability is relatively high. This is expected based on the user activity, since when the PU is at low duty cycle, the false alarm probability should be low while a relatively higher miss detection probability can be tolerated (note that it is not possible to let both be low).

Table 1: The comparison of  $\gamma$  and  $P_e^i$  between theoretical and simulation (denoted as ‘Sim’) results in Fig. 2.

$P(H_0)$	$\gamma$		$P_e^i$	
	Theoretical	Sim	Theoretical	Sim
0.1	49.7119	50	0.0303	0.0305
0.2	51.8787	52	0.0546	0.0556
0.3	52.4793	52	0.0767	0.0769
0.4	53.2524	53	0.0858	0.0861
0.5	54.1804	54	0.0908	0.0907
0.6	55.2552	55	0.0846	0.0848
0.7	56.5407	57	0.0745	0.0749
0.8	58.2112	58	0.0597	0.0598
0.9	60.8281	61	0.0381	0.0383

Next, the impact of noise on the total error probability is examined. The configurations are the same as in the first scenario, except that the noise variances  $\sigma_i$  are randomly generated as Gaussian distribution with variance 2, referred to as the *heavily noisy* environment. Fig. 3 illustrates three probabilities,  $P_f$ ,  $P_m$ , and  $P_e$ . It can be seen that all probabilities in a heavily noisy environment are bigger than those in a moderately noisy environment. To illustrate the shape of  $P_e$  and the existence of the minimum of  $P_e$ , extensive simulations are conducted. Figs. 2 and 3 have shown six representative scenarios. The results in other scenarios are similar to those in Figs. 2 and 3 with regard to the shape of  $P_e$  and the existence of the minimum of  $P_e$ , i.e., the  $P_e$  always first decreases until it reaches a minimum point,

and then increases. Due to the space limit, the illustration of the results for other scenarios is omitted.

For comparative purpose, the performance of generic cooperative spectrum sensing, equal weighted cooperative sensing (a special case of the proposed scheme in which all SUs are assumed the same weight), and the SNR-based weighted cooperative sensing from [27] have also been evaluated. Fig. 4 shows the total error probabilities of these schemes compared with the proposed scheme. The generic cooperative spectrum sensing has the highest error probability. This is because its false alarm probability dramatically increases while its miss detection probability smoothly decreases. The proposed scheme outperforms all other schemes, including the SNR-based weighted cooperative scheme in [27]. The performance gain is more significant in Fig. 4(b). This implies that the proposed scheme is more robust to, or less impacted by, the heavily noisy environment than other schemes.

Fig. 4 also demonstrates the impact of the PU activity on the total error probability. Intuitively, the total error probability is expected to be high at  $P(H_0) = 0.5$ . This is because it is prone to making an incorrect decision when the channel alternates the status equally. On the other hand, a correct decision is likely to be made when the channel stays idle (or occupied) with a high probability, which is shown on the figure where the total error probability approaches 0 when  $P(H_0)$  is close to 0 or 1.

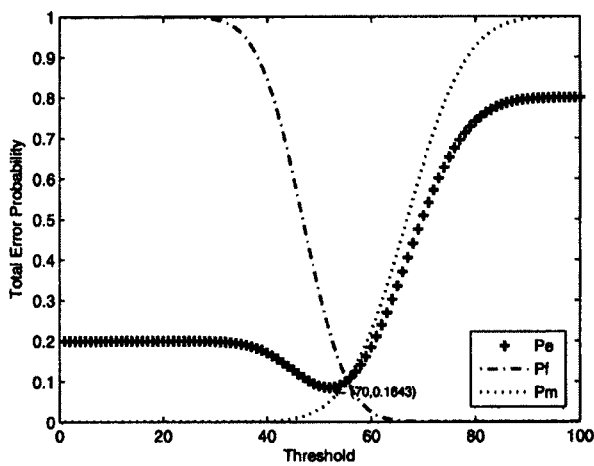
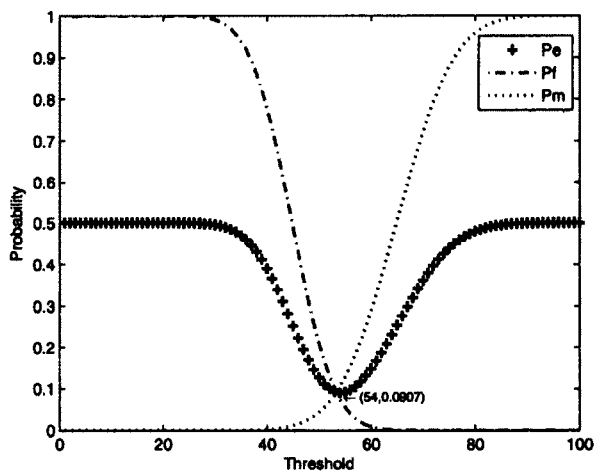
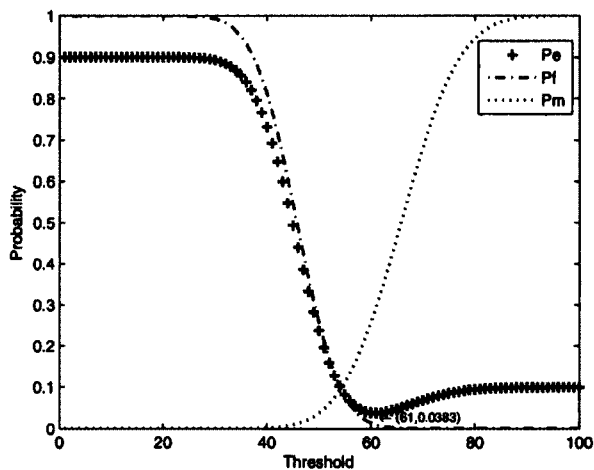
At last, the impact of the number of SUs on the total error probability is examined. Fig. 5 shows that the total error probability,  $P_e$ , decreases when the number of SUs participating in the cooperative sensing increases from 1 to 15 for a given  $P(H_0)$ . That is,  $P_e$  is a non-increasing function with respect to the number of SUs. Therefore, for a given maximum tolerable error probability, only a fraction of SUs participate in cooperative sensing.

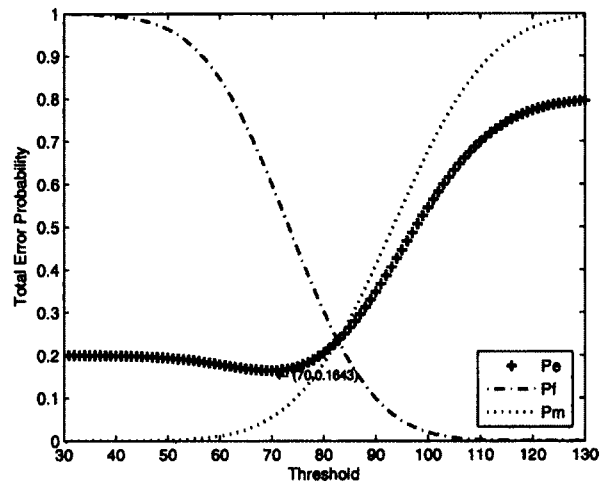
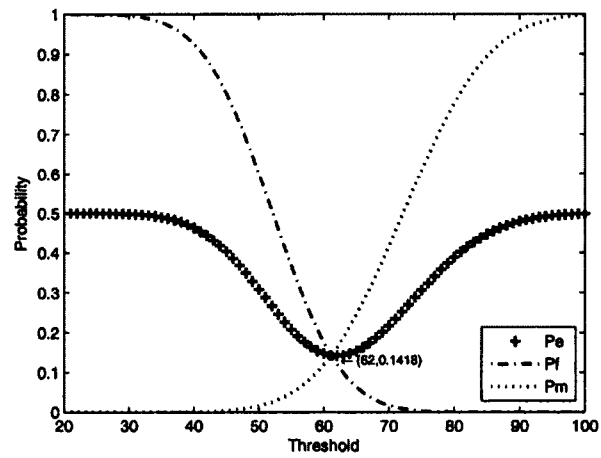
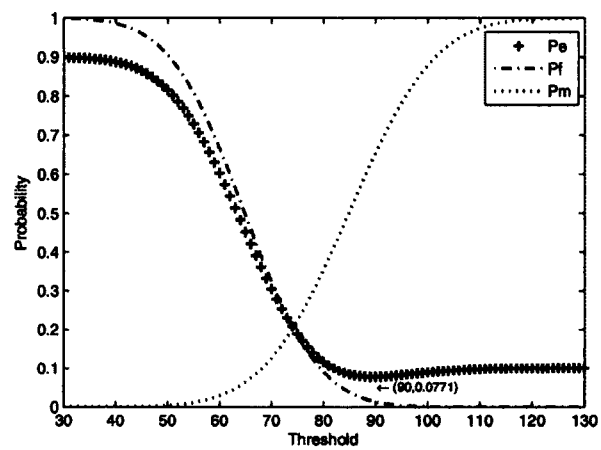
Fig. 6 shows the minimum number of SUs required to participate in cooperative sensing for a given maximum tolerable error probability ( $\epsilon$ ). In this scenario, 20 SUs are assumed in the network. It can be seen that for a moderately tolerable error probability, much fewer than 20 SUs are needed to participate in cooperative sensing. For example, if  $\epsilon = 0.08$ , then the number of SUs required to participate in cooperative sensing are 5, 8, and 10 when  $P(H_0) = 0.1, 0.3, \text{ and } 0.5$ , respectively.

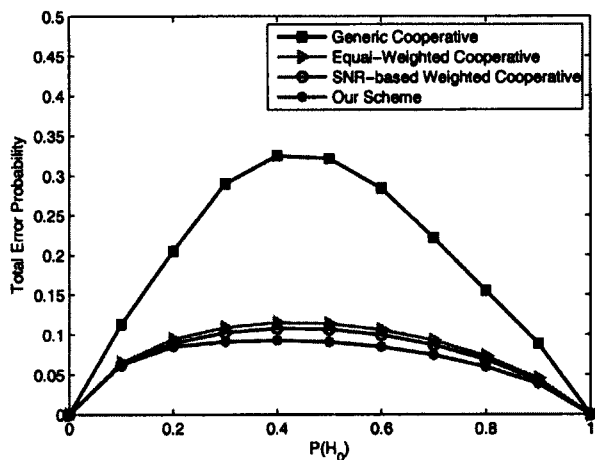
#### **III.4 SUMMARY**

A weighted cooperative spectrum sensing framework has been proposed. The total error probability, which combines the false alarm probability and miss detection probability, is defined to measure the detection accuracy. In addition, a theoretical model for the proposed weighted cooperative spectrum sensing is proposed, and the optimal detection threshold is derived. The number of SUs required to participate in cooperative sensing, subject to a given total error probability, is also studied.

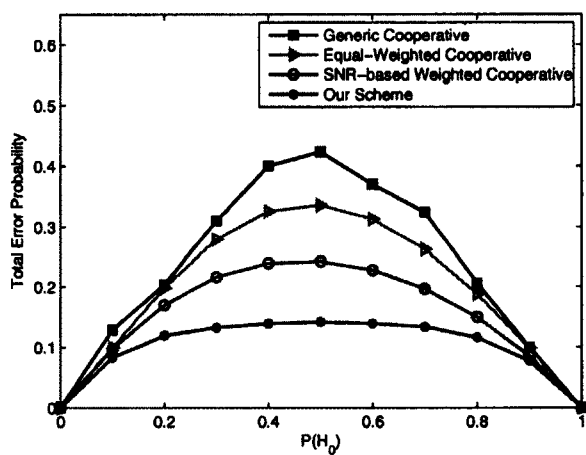


(a)  $P(H_0) = 0.2, P(H_1) = 0.8$ (b)  $P(H_0) = 0.5, P(H_1) = 0.5$ (c)  $P(H_0) = 0.9, P(H_1) = 0.1$ Fig. 2:  $P_f, P_m$  and  $P_e$  under the moderately noisy environment

(a)  $P(H_0) = 0.2, P(H_1) = 0.8$ (b)  $P(H_0) = 0.5, P(H_1) = 0.5$ (c)  $P(H_0) = 0.9, P(H_1) = 0.1$ Fig. 3:  $P_f, P_m$  and  $P_e$  under the heavily noisy environment



(a) Performance under the moderately noisy environment



(b) Performance under the heavily noisy environment

Fig. 4: Comparison of the total error probability

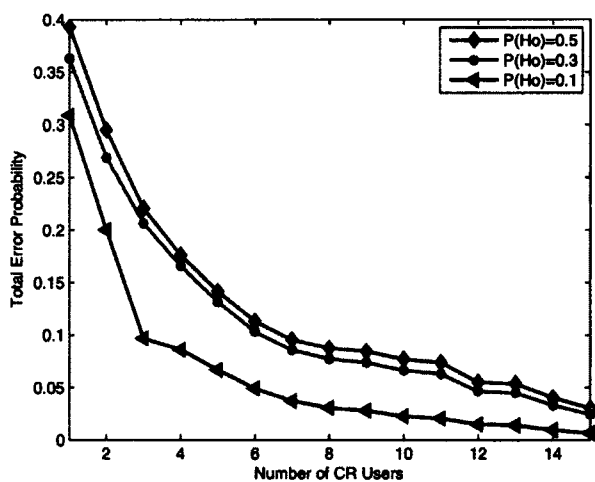


Fig. 5: The total error probability with different number of SUs.

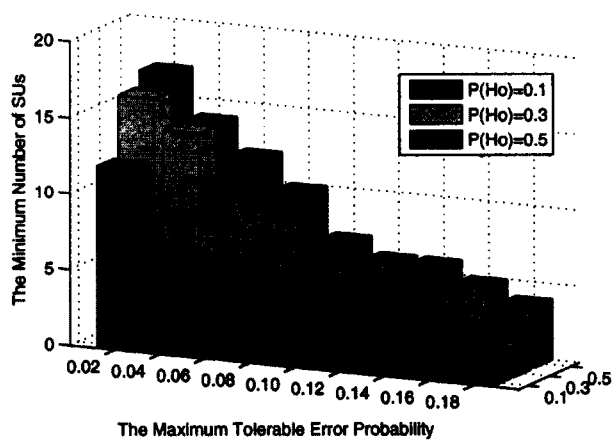


Fig. 6: The minimum number of SUs ( $m$ ) required to the maximum tolerable error probability ( $\epsilon$ )

## CHAPTER IV

### SENSING TECHNOLOGY FOR THREE-STATE SENSING MODEL

Chapter III examined spectrum sensing in a single CRN. This chapter will shift the attention on spectrum sensing from a single CRN to multiple co-existing CRNs. In fact, in most of the existing spectrum sensing literature, the system model constitutes a single CRN. Meanwhile, the primary focus is to detect the existence of signals on a channel, i.e., classify the channel into *idle* or *busy*, referred to as a two-state model, which is described as Eq. 2 in Section III.1. Based on this two-state model, any captured signal is identified as a PU's signal. Otherwise the channel is determined as idle. This model works properly with a single infrastructure-based CRN, in which the base station (BS) can easily notify its SUs not to conduct sensing process if an SU is transmitting data. Thus, from the perspective of SUs in a single CRN, there are only two channel states.

In practical systems, not one, but multiple CRNs operate together. The two-state model is insufficient for such a system. Consider a scenario that a channel might be occupied by an SU from one CRN and therefore SUs in other CRNs misinterpret this channel as occupied by the PU. When there is a considerably large number of available idle channels, whether a channel is occupied by a PU or an SU is trivial. SUs can simply switch to other idle channels. However, with the rapid proliferation of various wireless applications, the number of SUs typically exceeds the number of idle channels. In this case, it is essential to determine whether a PU or an SU is using the channel. The reason is that if SUs in one CRN are continuously accessing the channel, then SUs in other CRNs would detect the channel as busy and hence starve. To solve this problem, a smart sensing model, i.e.,

a three-state sensing model, is invented which consists of  $H_0$  (*idle*),  $H_1$  (*occupied by a PU*) and  $H_2$  (*occupied by an SU*). This three-state sensing model effectively addresses the fairness concern of the two-state model, and resolves the starvation problem of multiple co-existing CRNs.

With this smart sensing model, a fundamental question is raised: how to effectively detect each of the three states. This task is not straightforward, since distinguishing  $H_1$  from  $H_2$  is highly challenging. Feature sensing seems a promising way to achieve this objective. However, this method strongly depends on specific signals and it is not trivial to get such a feature. Currently, only TV band signal provides detailed signature information. For other bands being released, it is possible to get the signature information, but more investigation is needed. In this chapter, a novel solution to differentiate between  $H_1$  and  $H_2$  is proposed. The methodology is a two-stage detection procedure. In the first stage, energy detection is employed to identify whether the channel is idle or not. If the decision metric is lower than a predefined threshold, the channel is considered *idle* ( $H_0$ ). Otherwise, the channel is considered occupied, but, at this point, it is not clear whether a PU or an SU is using the channel. Received signal is further analyzed at the second stage that is based on a distance estimation technique, with an objective to make a final decision of either  $H_1$  or  $H_2$ . For the second stage, a statistical model is developed for distance estimation. For detection performance, the false alarm and miss detection probabilities for our spectrum sensing technology are theoretically analyzed in both local and cooperative sensing scenarios.

The rest of the chapter is organized as follows. Section IV.1 presents the network model and methodology. In Section IV.2, the detailed design of the proposed spectrum sensing framework is presented along with in-depth analysis. The numerical results are presented

in Section IV.3. Concluding remarks are drawn in Section IV.4.

## IV.1 THREE-STATE SENSING MODEL AND METHODOLOGY

### IV.1.1 THREE-STATE SENSING MODEL

The traditional two-state model, which is predominantly used in the existing spectrum sensing methods, is re-written as follows:

$$r_i = \begin{cases} n_i, & H_{idle} \\ x + n_i, & H_{busy} \end{cases}, \quad (27)$$

where  $r_i$  is the signal that the  $i^{\text{th}}$  SU received,  $n_i$  is the zero-mean additive white Gaussian noise (AWGN), i.e.,  $n_i \sim \mathcal{N}(0, \sigma_i^2)$  and  $x$  is the signal that a user transmits. Note that the channel gain is ignored because it is often assumed to be constant during the detection interval.

This two-state model works properly with a single infrastructure-based CRN. Nevertheless, as pointed out in Section IV, it is insufficient with multiple CRNs co-existing in an area. Consider a system with one PU, denoted by  $PU$ , coupled with multiple infrastructure-based cognitive radio networks, denoted as  $CRN_1, CRN_2, \dots, CRN_M$ . For the  $i^{\text{th}}$  CRN, it consists of  $N_i$  SUs. SUs inside the same network associate with a dedicated base station, denoted as  $BS_i$ .  $BS_i$  is responsible for control information broadcasting, transmission scheduling, and so on, within the same network. Note that there are no direct communications among BSs from distinct networks. All CRNs opportunistically share a licensed channel with the PU for data transmission.

Since BSs from distinct CRNs are not able to communicate with each other, it is highly

likely that an SU from one CRN is using the channel when SUs from other CRNs detect the channel as busy. Given a system with one PU and two co-existing CRNs, assume one SU from  $CRN_1$  is transmitting data on the licensed channel. Then other SUs inside  $CRN_1$  will be notified by  $BS_1$  that an SU is using the channel and hence not to perform spectrum sensing. In contrast, the SUs in  $CRN_2$  are unaware of this. They implement regular spectrum sensing process. As a result, the channel is detected as busy, which means  $CRN_2$  incorrectly believes that the channel is occupied by the PU, and thus  $CRN_2$  is prohibited to access the channel. As a conclusion, a channel will often be wrongly determined as “occupied by a PU” as long as any SU is accessing the channel. This results in significantly high false alarm probability. To more accurately reflect the channel states with co-existing multiple CRNs, a three-state sensing model is proposed which consists of  $H_0$  (*idle*),  $H_1$  (*occupied by a PU*) and  $H_2$  (*occupied by an SU*) defined as follows:

$$r_i = \begin{cases} n_i, & H_0 \\ x_p + n_i, & H_1 \\ x_s + n_i, & H_2 \end{cases}, \quad (28)$$

where  $x_s$  is the signal that an SU transmits and  $x_p$  is the signal that a PU transmits. All the other notations follow the same meaning as in the two-state model.

In fact,  $CRN_2$  should take different actions depending on whether the detection result is  $H_1$  or  $H_2$ . Specifically, if the channel is actually *occupied by the PU* ( $H_1$ ),  $CRN_2$  is prohibited from transmission. On the contrary, if the channel is accessed by an SU in  $CRN_1$  ( $H_2$ ),  $CRN_2$  is allowed to stay and compete for the channel. It is noteworthy that a channel is considered as “*idle*” only after sensing a relatively long idle period. This period is defined as “sensing time”. So if the detection result is  $H_1$ , the very short idle intervals between two



successive transmission of PU frames are not treated as an “idle” state. In other words, SUs are prohibited to transmit data during those intervals. However, if an SU grasps a channel, the SUs from other CRNs are allowed to compete with it for access to the channel, even though the current SU still has data to transmit.

After addressing the significance of the distinction between  $H_1$  and  $H_2$ , a fundamental and challenging question is immediately raised: how to clearly and accurately detect the channel state from  $H_0$ ,  $H_1$  and  $H_2$ ? This question presents the primary motivation of this chapter and a solution to this problem will be solved in the following sections.

#### **IV.1.2 METHODOLOGY:TWO-STATE DETECTION PROCEDURE**

The methodology is a two-stage detection procedure. In the first stage, energy detection is utilized. The signal energy is assumed reasonably higher than the noise level and hence the detection accuracy of energy detection is fairly satisfactory. If the decision metric is lower than a predefined threshold, the channel is believed as idle ( $H_0$ ). Otherwise, the channel is considered occupied, but at this point it is not clear whether the PU or an SU is using the channel. Received signal is further analyzed by the second stage based on a distance estimation technique designed in Section IV.2. The second stage will make a final decision of  $H_1$  or  $H_2$ .

#### **IV.2 IMPLEMENTATION OF TWO-STATE DETECTION**

For the first stage, energy detection has been well studied and readers are referred to [23, 48] for the details. The primary concentration is focused on the second stage, which aims to effectively differentiate the PU’s signals from SUs’. Distance estimation is a promising

approach to accomplish this. Normally, PUs are physically protected according to FCC policy. For instance, IEEE 802.22 states that there is a protected contour of TV stations. In this system model,  $D_p$  is assumed as the radius of the protected area centered at the PU. Assume SUs have the location knowledge of both themselves and the PU. The location of the PU is denoted as  $(x_0, y_0)$  and the location of the  $i^{\text{th}}$  SU is denoted as  $(x_i, y_i)$ . Apparently, the real distance between the PU and the  $i^{\text{th}}$  SU, denoted as  $D_i$ , can be directly obtained as:  $D_i = \sqrt{(x_i - x_0)^2 + (y_i - y_0)^2}$ .  $P_T$  is the transmitted power from the PU and this information can be learned in advance. The received power can be measured at each SU. However, from the perspective of the transmitted power, SUs are unlikely to determine the signal source ahead of time. That is, SUs do not have the knowledge of the actual transmitted power. The signal was hypothesized from the PU and therefore the transmitted power equals  $P_T$ . From both the transmitted power and the received power, the  $i^{\text{th}}$  SU estimates the propagation distance, which is denoted as  $\hat{d}_i$ . A decision rule will be designed via comparing  $\hat{d}_i$  and  $D_i$  to determine whether the signal truly originates from the PU or not.

#### IV.2.1 STATISTICAL MODEL FOR PROPAGATION DISTANCE

It is not trivial to estimate a propagation distance with the knowledge of the transmitted and received powers only. Due to the complex and varied terrains, plus the uncertainty of noise, a deterministic model is not appropriate. However, there is no existing work which statistically models a propagation distance. Instead, the received power has been investigated extensively. In the following discussion, a solution to the propagation distance will be sought from a signal propagation model. A common statistical model for path-loss

propagation in dB is adopted as follows [49]:

$$P_R(\hat{d}_i) = P_T - \bar{L}(\hat{d}_i) - X_{\sigma_i}, \quad (29)$$

where  $P_R(\hat{d}_i)$  is the received power,  $\bar{L}(\hat{d}_i)$  is average value of the propagation path loss;  $X_{\sigma_i}$  follows a normal distribution with zero mean and standard deviation  $\sigma_i$  (2-6 dB). Okumura's Model is widely used for urban areas to estimate signal propagation. Okumura's model is used to obtain  $\bar{L}(\hat{d}_i)$  from the following expression:

$$\bar{L}(\hat{d}_i) = L_F(\hat{d}_i) + A_{mu}(f) - G(h_t) - G(h_r) - G_{AREA}, \quad (30)$$

where  $L_F$  is the free space propagation path loss;  $A_{mu}$  is the median attenuation relative to free space;  $G(h_t)$  is the PU antenna height gain factor;  $G(h_r)$  is the SU antenna height gain factor and  $G_{AREA}$  is the correction factor again due to the type of environment. In order to find out how to choose suitable values for  $A_{mu}$  and  $G_{AREA}$  according to a specific environment, readers are referred to [49].

The path loss for the free space model in dB is:

$$L_F(\hat{d}_i) = 20\log(\hat{d}_i) - 10\log\left(\frac{G_t G_r \lambda^2}{(4\pi)^2}\right), \quad (31)$$

where  $G_t$  is the PU antenna gain in the direction of the receiver and  $G_r$  is the SU antenna gain in the direction of the transmitter. Calculating using Eq. 29, 30 and 31, the term containing  $\hat{d}_i$  can be derived as follows:

$$20\log(\hat{d}_i) = C_i - (P_R(\hat{d}_i) + X_{\delta_i}), \quad (32)$$

where  $C_i$  can be treated as a constant and derived as follows:

$$\begin{aligned} C_i = & P_T - A_{mu}(f) + G(h_t) + G(h_r) \\ & + G_{AREA} + 10\log\left(\frac{G_t G_r \lambda^2}{(4\pi)^2}\right) \end{aligned} \quad (33)$$

At this point, the distribution of  $\hat{d}_i$  can be found and analyzed from Eq. 32. Note that the received power  $P_R(\hat{d}_i)$  in Eq. 32 is treated as a constant and is replaced by the measured received power, denoted by  $\widetilde{P}_i^R$ . As a consequence, the estimation of propagation distance  $\hat{d}_i$  can be expressed as follows:

$$20\log(\hat{d}_i) \sim N(C_i - \widetilde{P}_i^R, \delta_i^2), \quad (34)$$

It can be seen that  $\hat{d}_i$  follows a Gaussian distribution statistically. This model will be used to analyze the propagation distance with the transmitted and received power known.

#### IV.2.2 LOCAL SPECTRUM SENSING BASED ON DISTANCE ESTIMATION

Local spectrum sensing is a good starting point to explore the spectrum sensing technology. In this subsection, the sensing with an individual SU is first examined based on the distance estimation model in Eq. 32.

After getting the distribution of  $\hat{d}_i$  from Eq. 8, a threshold is needed to make a decision whether the received signal is from PU or not. Let  $\gamma_i$  denote the threshold. If the signal is from the PU,  $\hat{d}_i = D_i$  in an ideal situation. Thus, it is reasonable to conclude that the signal is from the PU if  $\hat{d}_i$  is close to  $D_i$ . Specifically, if  $|\hat{d}_i - D_i| < \gamma_i$ , the SU makes a decision of  $H_1$ . Otherwise, the detection result is  $H_2$ .

False alarm probability and miss detection probability are two significant metrics to evaluate the detection accuracy. Let us first examine the false alarm probability, denoted by  $P_f(i)$ . False alarm means that the signal from an SU is wrongly interpreted as a PU signal.

**Theorem 1:** Given a threshold  $\gamma_i$ , the false alarm probability  $P_f(i)$  is:

$$P_f(i) = \left(1 - \frac{\alpha + \beta}{2\pi}\right) \left( Q\left(\frac{C_i - \widetilde{P}_i^R - 20\log(D_i + \gamma_i)}{\delta_i}\right) - Q\left(\frac{C_i - \widetilde{P}_i^R - 20\log(D_i - \gamma_i)}{\delta_i}\right) \right), \quad (35)$$

where  $\alpha$  and  $\beta$  are referred to Fig. 7.

*Proof.* Suppose that the signal source is determined as the PU. From the distribution expression in Eq. 34, the conditional detection probability, denoted as  $P_1(i)$  can be found as follows.

$$\begin{aligned} P_1(i) &= Pr[|\widehat{d}_i - D_i| < \gamma_i] \\ &= Pr[-\gamma_i < \widehat{d}_i - D_i < \gamma_i] \\ &= Pr[20\log(D_i - \gamma_i) < 20\log(\widehat{d}_i) < 20\log(D_i + \gamma_i)] \\ &= Q\left(\frac{C_i - \widetilde{P}_i^R - 20\log(D_i + \gamma_i)}{\delta_i}\right) \\ &\quad - Q\left(\frac{C_i - \widetilde{P}_i^R - 20\log(D_i - \gamma_i)}{\delta_i}\right), \end{aligned} \quad (36)$$

where  $Q(x)$  is a Q-function.

Eq. 36 works based on the hypothesis that the signal is from the PU. As a matter of fact, it might not be accurate that the signal is from the PU merely with an estimated distance. Fig. 7 renders an explanation of this. In Fig. 7,  $D_p$  is the radius of the protected area.  $|\widehat{d}_i - D_i| < \gamma_i$  is reflected into a whole ring. The larger radius of the ring is denoted as  $R_2$ , which equals  $(D_i + \gamma_i)$ . The smaller radius of the ring is denoted as  $R_1$ , which equals  $(D_i - \gamma_i)$ . Note that only half of the ring is drawn and shaded. The overlapped area between the shaded ring and the circle with a radius  $D_p$  is considered that the signal originates from

the PU. The corresponding probability of the overlapped area relative to the whole ring can be approximately derived as:

$$P_2(i) = \frac{\alpha + \beta}{2\pi}, \quad (37)$$

where  $\alpha$  and  $\beta$  are radians and satisfy:

$$\cos \alpha = \frac{D_i^2 + R_2^2 - D_p^2}{2D_i R_2}, \quad \sin \beta = \frac{D_p}{D_i}.$$

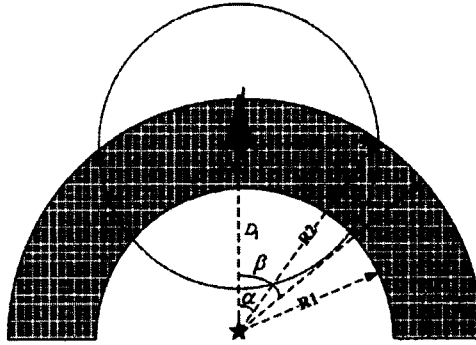


Fig. 7: Distance estimation with a single SU (represented by the solid star)

By the definition of the false alarm, it is from the ring area except the overlapped portion.

So, the false alarm probability  $P_f(i)$ , is represented as:

$$\begin{aligned} P_f(i) &= P_1(i) * (1 - P_2(i)) \\ &= \left(1 - \frac{\alpha + \beta}{2\pi}\right) \left(Q\left(\frac{C_i - \widetilde{P}_i^R - 20\log(D_i + \gamma_i)}{\delta_i}\right) - Q\left(\frac{C_i - \widetilde{P}_i^R - 20\log(D_i - \gamma_i)}{\delta_i}\right)\right) \end{aligned}$$

□

Another critical metric is the miss detection probability, denoted by  $P_m$ . On the contrary to  $P_f(i)$ , miss detection probability means that the signal of PU is incorrectly determined as an SU's. Next this will be theoretically analyzed.

**Theorem 2:** Given a threshold  $\gamma_i$ , the miss detection probability is:

$$\begin{aligned}
 P_m(i) &= \left(1 - \frac{4\gamma_i(\alpha + \beta)}{2\pi D_p}\right) \left(1 - Q\left(\frac{C_i - \widetilde{P}_i^R - 20\log(D_i + \gamma_i)}{\delta_i}\right)\right) \\
 &\quad + Q\left(\frac{C_i - \widetilde{P}_i^R - 20\log(D_i - \gamma_i)}{\delta_i}\right)
 \end{aligned} \tag{38}$$

*Proof.* Miss detections occur with two conditions. One is that the estimated location of the PU falls within the circle area centered at the PU with a radius of  $D_p$ . The second is that  $|\widehat{d}_i - D_i| > \gamma_i$ . Let us calculate the probability of the first condition, denoted as  $P_3(i)$ . Specifically,  $P_3(i)$  is referred to as a fraction. The numerator is the circle area subtracting the overlapped area between the circle and the ring in Fig. 7. The denominator is the whole circle area. Therefore,

$$\begin{aligned}
 P_3(i) &= 1 - \frac{(D_p + \gamma_i)^2 - (D_p - \gamma_i)^2}{D_p^2} \cdot \frac{\alpha + \beta}{2\pi} \\
 &= 1 - \frac{4\gamma_i}{D_p} \cdot \frac{\alpha + \beta}{2\pi}
 \end{aligned} \tag{39}$$

In addition, the probability of  $|\widehat{d}_i - D_i| > \gamma_i$  can be obtained from Eq. 36 easily as:

$$Pr(|\widehat{d}_i - D_i| > \gamma_i) = 1 - P_1(i). \tag{40}$$

Combining Eq. 39 and Eq. 40, the miss detection probability can be written as:

$$\begin{aligned}
 P_m(i) &= P_3(i) \cdot Pr(|\widehat{d}_i - D_i| > \gamma_i) \\
 &= \left(1 - \frac{4\gamma_i(\alpha + \beta)}{2\pi D_p}\right) \left(1 - Q\left(\frac{C_i - \widetilde{P}_i^R - 20\log(D_i + \gamma_i)}{\delta_i}\right)\right) \\
 &\quad + Q\left(\frac{C_i - \widetilde{P}_i^R - 20\log(D_i - \gamma_i)}{\delta_i}\right)
 \end{aligned}$$

□

After calculating both the false alarm and miss detection probabilities, it is time to analyze the critical parameter, threshold  $\gamma_i$ . It is commonly acknowledged that there is an inherent trade-off relationship between  $P_f(i)$  and  $P_m(i)$ . The threshold is expected to reduce both  $P_f(i)$  and  $P_m(i)$  as low as possible. One possible approach to obtain the threshold  $\gamma_i$  is to set  $P_f(i) = P_m(i)$ . The threshold  $\gamma_i$  can also be achieved to meet some specific detection requirements, for example,  $P_f(i) \leq \zeta$  or  $P_m(i) \leq \zeta$ , where  $\zeta$  is a constant and  $0 < \zeta < 1$ . Depending on the specific requirement,  $\gamma_i$  can be obtained accordingly.

### IV.2.3 COOPERATIVE SPECTRUM SENSING AMONG SUS

The previous subsection introduced sensing with an individual SU. However, a single SU is not accurate enough to distinguish the signal from the PU. This is because all locations on the circle edge with a radius of the estimated distance are possible signal sources. Fig. 7 has depicted this situation. Two SUs are not sufficient to distinguish the signal, either. This is interpreted as in Fig. 8(a), where the solid stars represent SUs. It can be seen that the two circles, centered at each SU, have two intersection points, i.e., possible signal sources. One is the PU and the other is drawn as the solid dot, which is symmetric to the PU. In other words, two SUs are not able to determine the transmitter without ambiguity. Three SUs, described in Fig. 8(b), are capable of identifying a specific transmitter without ambiguity. So, at least three or more SUs are needed to cooperate.

On one hand, more SUs will enhance the detection accuracy. On the other hand, the computational complexity will be increased considerably. A cooperative spectrum sensing



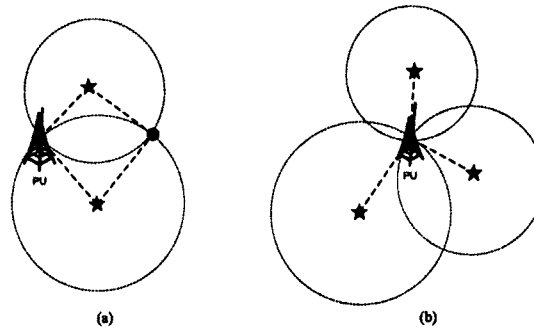


Fig. 8: Distance estimation with two SUs in (a): the solid stars represent SUs and the solid circle represents another possible single source, which is symmetric to the PU; and three SUs in (b): solid stars represent SUs and three of them can determine a specific transmitter without ambiguity.

scheme will be proposed with the objective of improving the detection accuracy. The basic idea is that a portion of SUs in the same CRN are chosen to conduct cooperative spectrum sensing. First, three SU leaders are selected. Afterwards, the neighbors within a given reference range, denoted by  $D_r$ , surround each leader, form a group. Finally, SUs of three groups will perform sensing cooperatively.

The selection of three SU leaders is a key issue and should follow two basic rules. First, the chosen SUs should not be physically located very far from the PU because the signal quality will decrease dramatically with the propagation distance. Second, the distance between any two of three leaders should not be very short, since the SUs that are physically close are prone to experience similar propagation quality. Obeying the first rule, an area with a radius  $D$  ( $D > D_p$ ) is defined, within which three leaders are chosen. To satisfy the second rule, two SUs with the largest distance are first selected, then a third one is chosen which is relatively far from both. The algorithm showing how to select three SU leaders, denoted by  $a$ ,  $b$  and  $c$ , is summarized in **Algorithm 2**:

After selecting three SU leaders, three respective groups are generated accordingly. SUs

---

**Algorithm 2** Selection of three SU leaders
 

---

- 1: Define a circle area with a radius  $D$  centered on the PU. Count the number of SUs in this area, denoted as  $M$ ,
  - 2: **for**  $i = 1:1:M$  **do**
  - 3:   **for**  $j = 1:1:M$  **do**
  - 4:      $D(i, j) = \sqrt{(x_i - x_j)^2 + (y_i - y_j)^2}$
  - 5:   **end for**
  - 6: **end for**
  - 7: Choose the two SUs with the largest distance, denoted as  $a$  and  $b$ , that is:  $D(a, b) = \max\{D(i, j)\}$
  - 8: Select the third SU, denoted as  $c$
  - 9: **for**  $i = 1:1:M-2$  (except  $a, b$ ) **do**
  - 10:    $\delta(a, b, i) = |D(a, i) - D(a, b)|/\sqrt{2}$
  - 11: **end for**
  - 12:  $\delta(a, b, c) = \min\{\delta(a, b, i)\}$
- 

within three groups first conduct local spectrum sensing based on distance estimation. Assume the total number of selected SUs is  $S_i$  in the  $i^{\text{th}}$  ( $i = 1, 2, 3$ ) group. These  $S_i$  SUs report the decision results, either  $H_1$  or  $H_2$ , to their SU leader by performing the ‘‘Half Voting’’ strategy. That is, the channel is determined as  $H_1$  only if over half of the results are  $H_1$ . Otherwise, the channel is considered as  $H_2$ . With this rule, let us investigate the cooperative false alarm probability  $P_f^{CO}$  and cooperative miss detection probability  $P_m^{CO}$  in a single group, respectively:

$$P_f^{CO}(i) = \sum_{k=S_i/2}^{S_i} \binom{S_i}{k} \prod P_f(k) \prod_{l \neq k}^{S_i-l} (1 - P_f(l)) \quad (41)$$

$$P_m^{CO}(i) = 1 - \sum_{k=S_i/2}^{S_i} \binom{S_i}{k} \prod (1 - P_m(k)) \prod_{l \neq k}^{S_i-l} P_m(l). \quad (42)$$

Afterwards, three SU leaders report their decisions, either  $H_1$  or  $H_2$ , to the BS. If all these three reports are  $H_1$ , the BS makes a decision of  $H_1$ . Otherwise the decision is  $H_2$ . The final false alarm probability  $Q_f$  and miss detection probability  $Q_m$  can be found as

follows.

$$Q_f = \prod_{i=1}^3 P_f^{CO}(i) \quad (43)$$

$$Q_m = 1 - \prod_{i=1}^3 (1 - P_m^{CO}(i)) \quad (44)$$

After conducting cooperation twice, once in a single group and once among three leaders, the false alarm probability  $Q_f$  and miss detection probability  $Q_m$  degrade significantly. The detection performance will be verified in Section IV.3.

### IV.3 NUMERICAL RESULTS

In this section, the detection performance, including the false alarm probability  $P_f$  and the miss detection probability  $P_m$ , are extensively examined. Both local and cooperative sensing scenarios are fully considered.

#### IV.3.1 LOCAL SPECTRUM SENSING SCENARIO

In the local spectrum sensing scenario, only one PU and one SU are involved.  $P_f$  and  $P_m$  are extensively evaluated in numerous cases and all the results have similar curves. One representative example of them is demonstrated in Fig. 9. The major parameters used in this experiment are illustrated in Table 2.

It can be seen that in Fig. 9, the false alarm probability  $P_f$  increases when the threshold increases. The miss detection probability  $P_m$ , however, decreases along with the threshold. This verifies the inherent trade-off relationship between  $P_f$  and  $P_m$ . Furthermore, this fits well with the physical meaning of the false alarm and miss detection. As demonstrated in

Table 2: Parameters for the numerical experiment

Parameter	Value
Frequency (f)	400 MHz
Transmitted Power ( $P_T$ )	20 dB
Distance (d)	15 km
Stand deviation ( $\sigma_i$ )	1
PU Antenna Height ( $h_t$ )	200 m
SU Antenna Height ( $h_r$ )	1 m
PU Antenna Gain ( $G_t$ )	1
SU Antenna Gain ( $G_r$ )	1

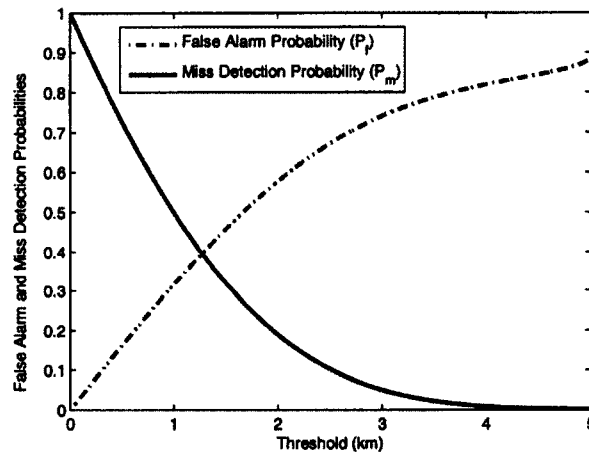
Fig. 9: The trade-off relationship between  $P_f$  and  $P_m$ 

Fig. 7 in Section IV.2.2, when the decision threshold  $\gamma_i$  increases, it is prone to incorrectly determine a signal is from the PU, and therefore  $P_f$  rises and  $P_m$  decreases.

### IV.3.2 COOPERATIVE SPECTRUM SENSING SCENARIO

In this subsection, the detection accuracy under the cooperative spectrum sensing scenario will be evaluated. Fig. 10 illustrates a sample network with 1 PU, 2 BSs and 150 SUs. SUs are randomly distributed and associated with 2 BSs as marked in the figure. The smaller circle centered at the PU is the protection area to the PU and the radius  $D_p$  is 2km.

The bigger circle is the area where the cooperative SUs are chosen from and the radius  $D$  is 10km.

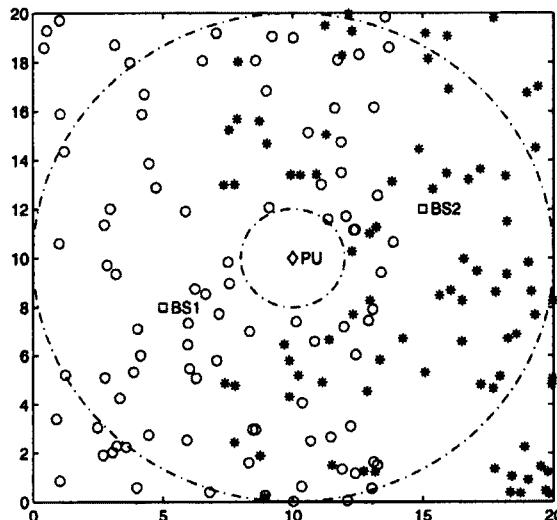


Fig. 10: Distribution of 1 PU, 2 BSs and 150 SUs in 2-D space. SUs are randomly distributed.

Essentially, the cooperative sensing is performed within one CRN. CRN2 depicted in Fig. 10 is taken as an example.  $D_r$  is set as 5km. Firstly,  $P_f$  and  $P_m$  are evaluated via “Half Voting” in one group. Secondly, three SU leaders further cooperate and obtain the corresponding  $Q_f$  and  $Q_m$ . The comparison is presented in Fig. 11. It can be seen that after conducting twice cooperations, the false alarm probability  $Q_f$  and miss detection probability  $Q_m$  degrade significantly in comparison with  $P_f$  and  $P_m$  in one group, given the threshold obtained when  $Q_f = Q_m$ .

#### IV.4 SUMMARY

In this chapter, the scenario of multiple CRNs co-existing in an area is taken into consideration. A smart three-state sensing model consisting of *idle*, *occupied by a PU* and

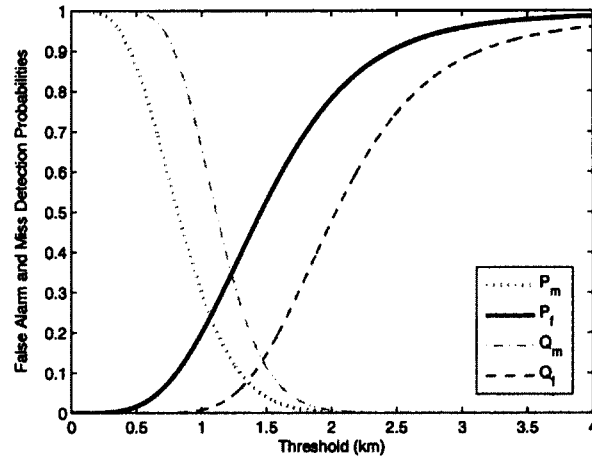


Fig. 11: Miss detection probability and false alarm probability:  $P_m$  and  $P_f$  is obtained in one group;  $Q_m$  and  $Q_f$  is further obtained with three leader SU.

*occupied by an SU* has been proposed in this scenario. To accurately detect each state of the three, a two-stage spectrum sensing methodology has been presented. For the second stage, a spectrum sensing approach based on statistical distance estimation technology have been designed. With this technology, both the local and cooperative spectrum sensing have been examined extensively.

## CHAPTER V

### USING SMART SENSING TO ACHIEVE FAIRNESS AMONG MULTI-CRNS

The smart sensing model, i.e., a three-state sensing model, has been previously proposed in Chapter IV. In this chapter, the performance of the three-state sensing model will be further analyzed. It is commonly acknowledged that fairness is a significant metric to evaluate the network performance. However, the fairness performance among SUs from multiple CRNs has received limited attention. In this chapter, how to using smart sensing to achieve fairness among SUs from multiple co-existing CRNs will be thoroughly examined. First, a MAC protocol is designed, termed *fairness-oriented media access control (FMAC)* protocol, based on the smart sensing model. The PU activity is fully considered in the design of FMAC, because PUs have strict priority over SUs and it is likely that they may appear or reappear at anytime. The goal of FMAC, together with the smart sensing model, is to achieve fairness among SUs from multiple CRNs co-existing in an area. In terms of fairness, this performance can be measured over a long time period (called long-term fairness) or over a relatively short time period (called short-term fairness). Unlike the conventional fairness metrics that are usually measured in a specific time period, the fairness dynamics from a short (micro-level) to a relatively long (macro level) time period is the primary concern.

In addition, the performance of FMAC, which embodies the smart sensing model, is carefully analyzed. A novel Markov chain is tailored to model FMAC, in which a renewal process is conducted when the PU reappears. Further, the access probability to the channel for SUs is derived from the Markov chain. Both throughput and fairness are carefully

explored. Numerical results show that FMAC is able to significantly improve the fairness of coexisting cognitive radio networks while maintaining a high throughput.

The rest of the chapter is organized as follows. Section V.1 presents the system model and states the problem. In Section V.2, the detailed design of the proposed fairness-achieved MAC protocol is introduced. Section V.3 explores the in-depth performance analysis including fairness, throughput and delay. The numerical results are presented in Section V.4. Concluding remarks are drawn in Section V.5.

## V.1 SMART SENSING MODEL

In this section, the smart three-state sensing model is addressed once again with an emphasis on fairness analysis. Consider a system with one PU, denoted by  $PU$ , coupled with multiple CRNs, denoted by  $CRN_1, CRN_2, \dots, CRN_M$ . Note that each CRN is assumed to consist of SUs only and for the  $i^{th}$  CRN, it has  $N_i$  SUs. Each SU is equipped with two radios. One is dedicated to sensing spectrum and the other is for data transmission exclusively. All CRNs opportunistically share the channel with the PU for data transmission. Spectrum sensing is a crucial step in CRN. Within the same CRN, a centralized device, i.e., a BS, is used. Multiple SUs inside the same CRN implement cooperative sensing and their BS makes a final decision on the channel state. For the details of cooperative sensing, readers are referred to [50] [51]. The requirement time of spectrum sensing is restricted by several factors such as hardware components, detection accuracy and so on. On one hand, longer sensing time brings higher detection accuracy. On the other hand, it results in relatively long delay. So, regulators impose a constraint on the required detection time. Take IEEE 802.22 as an instance; the required detection time is 2 seconds. Here the required detection time



is denoted by  $DT$ . This means SUs spend a period of  $DT$  to finally determine the channel state. In other words, the channel state is updated periodically and the detection result at  $(k+1)DT$  actually reflects the channel state at  $k \cdot DT$ . Furthermore, ideal spectrum sensing is assumed.

As pointed out in Chapter IV, the two-state model is insufficient for a multi-CRN coexisting system. Here, a straightforward quantitative example is illustrated. Given five SUs, which are from five different CRNs, one SU named  $SU_1$ , is capturing the channel and all the other four SUs falsely believe the channel is occupied by the PU and hence are restrained from transmission. As a result,  $SU_1$  will continue its transmission until the PU reappears or it has no more traffic. Let us assume this time period is  $500s$ . During this observed period of  $500s$ , the transmission time of  $SU_1$  is  $t_1 = 500s$  and others are 0. The fairness among 5 SUs can be further calculated using the Jain Index as follows:

$$J_{two-state} = \frac{(\sum_{n=1}^5 t_n)^2}{5 \cdot \sum_{n=1}^5 t_n^2} = \frac{1}{5}$$

It can be concluded the fairness would be worse with more CRNs.

From the above example, the two-state model results in an unfair channel allocation among SUs. To solve the unfairness problem, efforts are made in two directions. The first and foremost is the smart sensing model, which is represented in Eq. 28 as in Section IV.1. The distinction between the two-state and the three-state lies in that  $H_{busy}$  splits into  $H_1$  (occupied by a PU) and  $H_2$  (occupied by an SU). The second direction is an appropriate MAC protocol based on this model.

Applying such a smart sensing model into the above-mentioned example, even though  $SU_1$  is using the channel, other SUs are able to detect the channel is occupied by an SU

and they will compete with  $SU_1$ . If all five SUs have the same access probability, theoretically, they will be provided equal transmission opportunities with  $t_n = 100s(n = 1, 2, \dots, 5)$ . Therefore, the fairness among those 5 SUs can reach an ideal fairness of  $J_{three-state} = 1$ . In practice, due to a specific contention scheme, a sensing detection requirement and other issues, the achieved fairness of the three-state sensing model will be slightly less than 1, but significantly better than the fairness of the two-state model. This will be evaluated in the Section V.4.

## V.2 FMAC: FAIRNESS-ACHIEVED MAC DESIGN

FMAC is designed based on the proposed smart sensing model. In a MAC protocol, fairness refers to the measure of the ability of a MAC protocol to share a common channel equally among multiple users. In this section, the fairness performance will be evaluated from the perspective of time-based fairness. For instance, considering  $N$  users compete for the same channel, the ideal fairness will be achieved if each user is assigned the  $1/N$  proportional time over the total period observed.

Since PUs have strict priority over SUs, two distinct channel access methods for PUs and SUs are employed. To guarantee the privilege of PUs, when PUs have traffic to transmit, they will immediately transmit when the channel is idle. Since it takes a while for SUs to withdraw from the channel, the PU waits for a period up to *the tolerable maximum*, denoted by  $T_{max}$ , ( $T_{max} \leq 2DT$ ), when an SU captures the channel. Additionally, there are no idle intervals between two consecutive PU frames (or the idle interval is negligible). In other words, the PU will continue to capture the channel until there is no more traffic to transmit.

Prior to digging into the details of the MAC scheme for SUs, let us lay out the basic

principles, or, how an SU can appropriately respond to a distinct channel state. As addressed previously, there are three possible states at any time:  $H_0$ ,  $H_1$  and  $H_2$ . SUs take distinct actions based on these three states. Specifically, if the state of the channel is  $H_1$ , SUs keep silent and will continue to monitor the channel. Next, let us explore the states of  $H_0$  and  $H_2$  closely. If the channel state is determined as  $H_0$ , SUs access the channel immediately. In contrast, if the channel is detected as  $H_2$ , SUs learn that the channel is occupied by a SU instead of the PU. As a result, they will participate in competing for the channel. During transmission, SUs keep sensing the channel in every  $DT$  period. If the sensing result is  $H_0$  or  $H_2$ , SUs continue accessing the channel. However, they have to vacate the channel whenever the PU comes back. The main idea of the proposed MAC protocol is illustrated in the Fig. 12.

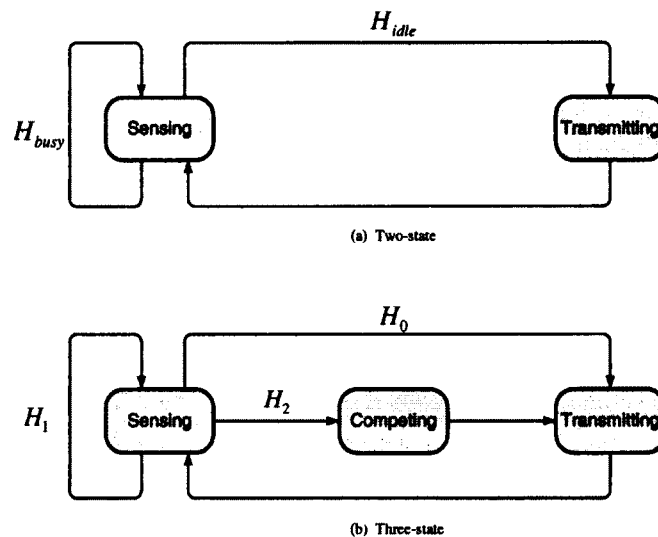


Fig. 12: Illustration of fairness-achieved MAC (FMAC) design with the two-state model shown in (a) and the three-state sensing model shown in (b).

Note that once an SU accesses an idle channel, in the views of other SUs, the channel state will be switched from  $H_0$  into  $H_2$ . Following how multiple SUs compete for the same channel under the state of  $H_2$  will be interpreted in details. The basic idea originates

from the IEEE 802.11 protocol, i.e., a backoff RTS/CTS scheme is employed. An SU monitors the channel activity when it has a packet to transmit. The SU starts transmitting only when an idle period equals a *Distributed Inter-Frame Space* (DIFS). Note that in the case of  $H_2$ , SUs do not need to wait for a period of  $DT$  as they do under the state of the  $H_0$ . In case the channel is busy, i.e., another SU is occupying the channel, the SU will randomly select a backoff interval from  $[0, W_c - 1]$ , where  $W_c$  represents the size of a contention window. The backoff time counter is decremented whenever the channel is sensed idle, stopped when a transmission is detected and reactivated when the channel is sensed idle again for a DIFS. Finally, the user transmits when the backoff time counter reaches 0. In case a collision occurs, i.e., two or more SUs transmit simultaneously, the same backoff technique is repeated. For the details of IEEE 802.11, readers are referred to [52]. Keep in mind that SUs continue sensing the channel during transmission or a backoff period and the PU may come back anytime. All SUs are expected to enter a renewal process whenever the PU reappears. In the renewal process, an SU randomly selects a backoff time from  $[0, W_c - 1]$  with an equal probability.

The fundamental differences between the proposed MAC protocol and IEEE 802.11 are two-fold. First, spectrum sensing is the unique feature of the CRNs and it is fully considered while designing the MAC protocol. According to the detection result, SUs take distinct actions as described previously. Secondly, the proposed MAC protocol is designed towards achieving fairness among SUs across multiple-CRNs. Recent studies pointed out that the fairness performance of IEEE 802.11 is not satisfactory [53]. The major reason is the binary exponential backoff technology. Based on such an exponential backoff technology, users that encounter collisions double their contention windows. As studied in [52], there is a

significant relation between the size of the contention window and the access probability. Users with a larger contention window have a relatively lower probability of access to the channel. As a matter of fact, the same access probabilities among competing users lead to the optimal fairness. Therefore, in order to achieve optimal fairness among SUs, the binary exponential backoff technology is not adopted. Instead, the same  $W_c$  will be used among all SUs and others remain the same as in IEEE 802.11.

### V.3 PERFORMANCE ANALYSIS

After introducing the detailed FMAC protocol, let us shift attention to the performance analysis of FMAC. Throughput and fairness are two crucial metrics and will be thoroughly examined in this section. To pave the road to their study, the PU activity which provides a statistical model is analyzed first. Second, FMAC is modeled as a Markov chain, from which the access probability of SUs is derived.

#### V.3.1 PU ACTIVITY ANALYSIS

This subsection analyzes the PU behavior concerned with the probabilities of the channel being idle and occupied by the *PU*. They are represented by  $P_0$  and  $P_1$ . One method to derive  $P_0$  and  $P_1$  is shown as Eq. 1 presented in Section III.1. This section provides a general method to derive  $P_0$  and  $P_1$ . Let  $X$  be a random variable that represents the time period that the PU transmits on the channel at once. Use the notation  $f_X(x)$  to denote the probability density function (pdf) for  $X$ .

With this PU model, Fig. 13 illustrates the PU traffic arriving time and the channel occupation by the PU and SUs. Let a random variable  $Y$  represent the period between two

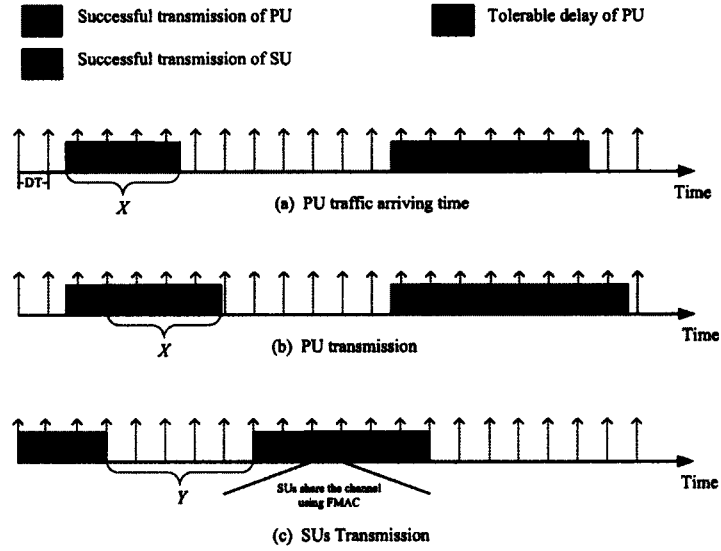


Fig. 13: PU activity modeling

consecutive SU transmission blocks, which is indicated in Fig. 13 (b). Carefully looking at (b) and (c) in Fig. 13, the following equation holds

$$Y = \left( \left\lceil \frac{X}{DT} + 1 \right\rceil \right) \cdot DT \cong X + DT. \quad (45)$$

Given the exponential distribution of  $X$ , let us derive the cumulative distribution function of  $Y$ , denoted by  $F_Y(y)$ .

$$F_Y(y) = Pr(x + DT < y) = \int_0^{y-DT} f_X(x) dx \quad (46)$$

Consequently, the pdf of  $Y$  can be written as:

$$f_Y(y) = F'_Y(y) \quad (47)$$

Let us observe a period of time  $t$ . After some calculations, the average of  $Y$ , denoted by  $E(Y)$  is expressed as:

$$E(Y) = \int_{DT}^{DT+t} y \cdot f_Y(y) dy \quad (48)$$

In this chapter, a specific distribution is taken as an example. Assume  $X$  follows an exponential distribution with a parameter, denoted by  $\mu$ . That is

$$f_X(x; \mu) = \mu \exp\{-\mu x\} \quad (49)$$

Then, the following equation holds:

$$f_Y(y) = F_Y'(y) = \mu \exp\{-\mu(y - DT)\} \quad (50)$$

and

$$E(Y) = \int_{DT}^{DT+t} y \cdot \mu \exp\{-\mu(y - DT)\} dz \cong \frac{1}{\mu} + DT \quad (51)$$

Additionally, the traffic from the PU is assumed to follow Poisson distribution with a parameter  $\lambda$ . So, the average arrivals of PU is  $\lambda \cdot t$ . Therefore,  $P_1$  can be obtained as

$$P_1 = \frac{\lambda \cdot t \cdot E(Y)}{t} = \left(\frac{1}{\mu} + DT\right) \cdot \lambda \quad (52)$$

Correspondingly,  $P_0$  can be achieved immediately as:

$$P_0 = 1 - P_1 \quad (53)$$

### V.3.2 SU ACCESS PROBABILITY

According to the proposed FMAC,  $W_c$  states from  $[0, W_c - 1]$  are modeled as the states in a Markov chain described in Fig. 14(a), in which the PU activity is fully taken into account. Following the transition probabilities is studied associated with this Markov chain. Each SU is assumed to always have a packet to transmit at any time. The number of SUs from multiple CRNs is considered as  $N$ . For a given time slot, there are four possible statuses, including PU occupation, successful SU transmission, idle and a collision among multiple

SUs. The probability of a PU occupation is actually  $P_1$ . The probability of successful SU transmissions, denoted by  $P_s(k)$ , can be derived as:

$$P_s = P_0 \cdot N \cdot P_a (1 - P_a)^{(N-1)}, \quad (54)$$

where  $P_a$  is the access probability of each SU. The derivation of  $P_a$  is postponed to the end of this subsection. The idle probability of a given time slot is:

$$P_i = P_0 \cdot (1 - P_a)^N. \quad (55)$$

The probability of collisions caused by multiple SUs, denoted by  $P_{cs}$  can be obtained as:

$$P_{cs} = P_0 \cdot (1 - (1 - P_a)^N - N \cdot P_a \cdot (1 - P_a)^{N-1}). \quad (56)$$

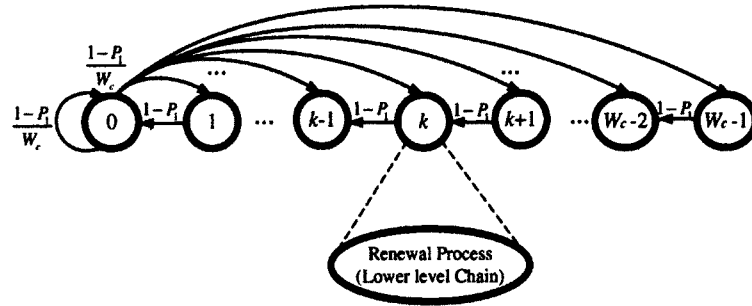
Note that SU transmissions only happen when the time counter reaches 0. Let us examine the state 0 first, which is followed by either a successful transmission with a probability  $(1 - P_1 - P_{cs})$ , a collision with a probability  $P_{cs}$ , or a collision with the PU with a probability  $P_1$ . In all cases, SUs need to wait for a randomly selected backoff time prior to the next transmission. Therefore the corresponding probability to choose any state from  $[0, W_c - 1]$  is

$$\frac{1 - P_1 - P_{cs}}{W_c} + \frac{P_{cs}}{W_c} + \frac{P_1}{W_c} = \frac{1}{W_c}.$$

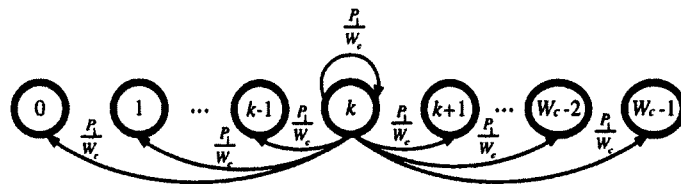
Now let us study the general case beside the state 0. Keep in mind that PU may reappear at any time and disturb a back off process. As a result, SUs may switch to a different channel in a multiple-channel scenario. It is reasonable to assume all SUs enter a renewal process whenever the PU comes back. In the renewal process, an SU randomly selects a backoff time from  $[0, W_c - 1]$  with a respective probability of  $\frac{P_1}{W_c}$ , which is described as a lower level chain in Fig. 14(a) and further interpreted in Fig. 14(b). Therefore, during a backoff period,



the time counter, e.g.  $k$ , can either decrease to  $(k - 1)$  with a probability of  $(1 - P_1)$ , or return to a renewal process with a probability of  $P_1$  once the PU re-appears.



(a) Two-level Markov Chain Model



(b) Renewal Process (Lower Level Chain)  
for a specific state  $k$

Fig. 14: (a) illustrates the transition probability among  $W_c$  states from  $[0, W_c - 1]$ , in which for each state it is possible to conduct a renewal process; (b) shows an example of the renewal process at a specific state  $k$ . Note that this renewal process applies to each state from  $[0, W_c - 1]$ .

Based on the above Markov chain model, one-step transition probabilities associated with the Markov chain can be written as follows. For any state  $k$  from  $[1, W_c - 1]$ , its preceding one  $(k - 1)$  is singled out to stress its distinction with others.

$$\begin{cases} P\{k/0\} = \frac{1 - P_1}{W_c} + \frac{P_1}{W_c} = \frac{1}{W_c}, k \in [0, W_c - 1] \\ P\{k-1/k\} = 1 - P_1 + \frac{P_1}{W_c}, k \in [1, W_c - 1] \\ P\{j/k\} = \frac{P_1}{W_c}, k \in [1, W_c - 1], j \neq k-1 \end{cases} ,$$

Following are the  $W_c$  balance equations of the Markov chain.

$$\begin{cases} \pi_0 = (1 - P_1 + \frac{P_1}{W_c}) \cdot \pi_1 + \frac{P_1}{W_c} (\sum_{i \neq 0} \pi_i), \\ (1 - \frac{P_1}{W_c}) \cdot \pi_k = \frac{1}{W_c} \cdot \pi_0 + \frac{P_1}{W_c} (\sum_{i \neq k} \pi_i), \quad k, i \in [1, W_c - 1] \end{cases}$$

After some calculations,

$$\begin{cases} \pi_0 = \frac{W_c - P_1}{W_c^2 - P_1} \\ \pi_k = \frac{W_c}{W_c^2 - P_1}, \quad k \in [1, W_c - 1] \end{cases}$$

Recalling that transmissions only occur at the state 0,  $\pi_0$  is actually the transmission probability of SUs, which is denoted as  $P_a$ . That is

$$P_a = \frac{W_c - P_1}{W_c^2 - P_1}. \quad (57)$$

Note that  $P_a$  is a significant parameter and will be used in the throughput analysis in V.3.3 and the fairness analysis in V.3.4.

### V.3.3 SU THROUGHPUT ANALYSIS

As for the throughput addressed in this subsection, only the throughput generated by SUs will be considered. We ignore the time periods of PU transmissions and merely concentrate on the SU s' throughput. Consequently, the throughput is calculated as:

$$\theta = \frac{P_s \cdot T_s}{P_i \cdot \sigma + P_s \cdot T_s + P_{cs} \cdot T_{cs} + P_1 \cdot T_{cp}}, \quad (58)$$

where  $\sigma$  is the duration of an empty slot time.  $T_s$  is the average time of a successful transmission,  $T_{cs}$  is the average time with a collision among SUs, and  $T_{cp}$  is the average time for a collision caused by the PU. Referring to [52],  $T_s$  and  $T_{cs}$  can be represented as follows by

means of the RTS/CTS Access mechanism:

$$\left\{ \begin{array}{l} T_s = RTS + SIFS + \delta + CTS + SIFS + \delta + H \\ + T_{DATA} + SIFS + \delta + ACK + DIFS + \delta \\ T_{cs} = DIFS + RTS + \delta \end{array} \right. \quad (59)$$

$T_{cp}$  is referred to the tolerable delay of the PU in Fig. 13 (b) and can be expressed as

$$T_{cp} = E[(1 + \tau) \cdot DT],$$

where  $\tau$  follows an uniform distribution from  $[0,1]$ . It is straightforward to derive  $T_{cp}$  as

$$T_{cp} = \frac{3}{2} \cdot DT, \quad (60)$$

The saturation throughput is the optimization of Eq. 58 and represented as:

$$\theta^* = \max\{\theta\} \quad (61)$$

It can be seen that several parameters such as  $W_c$ ,  $P_a$ ,  $P_1$ ,  $N$  and others play significant roles in the calculation of the throughput. Their impacts will be evaluated in the Section V.4.

Next, the distinction of the throughput will be discussed between the two-state and the three-state models. With the two-state model, SUs that compete for the channel belong to a single CRN. Instead, SUs from all CRNs have the opportunity to contend for the channel. The number of competing SUs increases in the three-state sensing model. As a result, with the same contention window  $W_c$ , the throughput may slightly degrade due to the increased collisions caused by more SUs. Nevertheless, the decrease is not considerable. Furthermore, the throughput reduction could be compensated by using an appropriate contention window. In other words, the three-state sensing model does not necessarily result in throughput reduction. This will be verified in Section V.4.

### V.3.4 FAIRNESS MEASUREMENT

In this section, the fairness performance among SUs across multiple CRNs will be examined in the perspective of time-based fairness. For convenience, “CRN” is used to represent “SUs from this CRN” hereafter unless otherwise specified. In the two-state model, two or more CRNs will attempt to use the channel simultaneously once the channel is detected idle and collisions may occur. As a result, they both believe the channel is occupied by the PU and give up the channel. After a random backoff time, the CRN that first comes back will transmit if no other CRNs appear in the following sensing time. Once a CRN grasps the channel, all other CRNs will be refrained from accessing the channel. In the three-state sensing model, the difference is that when two or more CRNs all sense the channel as idle, they will access the channel. They will further detect the signal is from a CRN and continue to access. Furthermore, if a CRN is using the channel, other CRNs can join to compete for the channel. In this way, all the SUs across multiple CRNs will achieve better transmission fairness via taking turns using the channel. Essentially, the three-state sensing model breaks the bounds of different CRNs and all SUs from multiple CRNs share the channel together.

Suppose  $N$  SUs contend for the channel access. Keep in mind these  $N$  SUs are from different CRNs. Let us examine the transmission fairness among them from a short to relatively long time period. Since no SUs are permitted to occupy the channel during the transmission of the PU, the period of PU transmission is ignored with regard to SUs’ fairness evaluation. But, we view the discontinuous time period (because of the disruption of PU transmission) as virtually continuous. Based on such a virtually continuous concept, a fixed time period is defined as a cycle and its length is denoted by  $\Delta_1$ . Assume  $K$  cycles are observed. SU’s actual transmission time in the accumulated time period, from  $\Delta_1$  (the

period of the first cycle),  $\Delta_2$  (the period of the first two cycles), ... till  $\Delta_K$  (the period of the first  $K$  cycles), is recorded in a matrix, denoted as  $\vec{\mathbf{T}}$ , as follows:

$$\vec{\mathbf{T}} = \begin{bmatrix} T_1(\Delta_1) & \cdots & T_1(\Delta_k) & \cdots & T_1(\Delta_K) \\ \vdots & \vdots & \vdots & \vdots & \vdots \\ T_n(\Delta_1) & \cdots & T_n(\Delta_k) & \cdots & T_n(\Delta_K) \\ \vdots & \vdots & \vdots & \vdots & \vdots \\ T_N(\Delta_1) & \cdots & T_N(\Delta_k) & \cdots & T_N(\Delta_K) \end{bmatrix},$$

where the element  $T_n(\Delta_k)$  represents the transmission time of the  $n^{\text{th}}$  SU during the period of  $\Delta_k$ .  $T_n(\Delta_k)$  is closely related to the access probability  $P_a$  as calculated in Eq. 57. Since all SUs share the same  $P_a$ , theoretically, they can reach an ideal fairness of 1. But, the simulation results will be slightly deviated from 1 and this will be verified in Section V.4.

In each time period, the traditional Jain Index fairness is calculated based on the corresponding column of  $\vec{\mathbf{T}}$ . Specifically, we calculate Jain Index in a vector expression as:

$$J(\vec{\mathbf{T}}(:,k)) = \frac{(\vec{\mathbf{1}} \cdot \vec{\mathbf{T}}(:,k))^2}{N \|\vec{\mathbf{T}}(:,k)\|^2}, \quad (62)$$

where  $\vec{\mathbf{T}}(:,k)$  is the  $k^{\text{th}}$  column vector in  $\vec{\mathbf{T}}$  and  $\vec{\mathbf{1}} = [1, 1, \dots, 1]$  is a  $1 \times N$  row vector whose elements are all 1. Note that the value of  $J$  ranges from 0 to 1. The larger the Jain Index, the better the transmission fairness among SUs. In the ideal case,  $J$  should be 1.

Jain Index in Eq. 62 is used to evaluate the transmission fairness during a specific time period. Nevertheless, the fairness dynamics from a short to a relatively long time are our principle concern. In order to examine the fairness from micro to macro level, in fact, several time periods ranging from  $\Delta_1$  to  $\Delta_K$  are involved. To better measure this, a metric termed ALFA is defined, which is essentially the average of Jain Index in all time periods.

Mathematically, ALFA, denoted as  $A(\vec{T})$ , is computed as:

$$A(\vec{T}) = \frac{1}{K} \sum_{k=1}^K J(\vec{T}(:,k)), \quad (63)$$

Obviously, ALFA falls into  $[0,1]$  and the larger ALFA, the better fairness from micro to macro level.

In the two-state model, it is highly likely that SUs from one CRN aggressively occupy the channel for a relatively long time and thus it is not fair to SUs from other CRNs. Instead, this situation will be avoided in the three-state sensing model. Therefore, SUs from different CRNs will achieve better fairness, from micro to macro level, through transmitting by turns. ALFA will be measured in Section V.4.

#### V.4 NUMERICAL RESULTS

In this section, the throughput and fairness performance will be evaluated extensively. We attempt to verify that fairness of the three-state sensing model is significantly improved, while maintaining a similar throughput compared to the two-state model. The major parameters used to run numerical results are listed in Table 3 .

Table 3: Major parameters for the numerical experiment

Parameter	Value
MAC header	272 bits
PHY header	128 bits
ACK	112 bits + PHY header
RTS	160 bits + PHY header
CTS	112 bits + PHY header
Channel Bit Rate	1 Mbits/s
Propagation Delay	1 $\mu s$
Slot Time	50 $\mu s$
SIFS	28 $\mu s$
DIFS	128 $\mu s$
DT	6000 $\mu s$

#### V.4.1 THROUGHPUT EVALUATION

In the first experiment, each CRN has 10 users and three scenarios, with 2, 3, and 4 co-existing CRNs, are studied, respectively. The PU activity is given as  $P_0 = 0.8$ . In Fig. 15, each curve represents the throughput of the two-state model or the three-state sensing model. For the two-state model, only one CRN is able to share the channel, so the number of SUs that compete for the channel is always 10 no matter how many multiple CRNs are co-existing. In contrast, for the three-state sensing model, with 2 co-existing CRNs, there are 20 SUs that share with the channel. With 3 co-existing CRNs, 30 SUs compete for the channel and so on. The throughput in each case is illustrated with a changing contention window size. The saturation throughput is reached when the throughput is maximized. Note that the optimal window size to maximize the throughput increases with the growth of competing SUs. From Fig. 15, we learn that the saturation throughput in each case is quite similar. To further verify this conclusion, Fig. 16 plots the saturation throughput of the two-state model and the three-state sensing model with 2 co-existing CRNs. This figure indicates the saturation throughput of the three-state merely slightly decreases compared to the result of the two-state.

In the second experiment, the impact of the PU activity on the SUs' throughput is explored. Fig. 17 clearly demonstrates that the saturation throughput of SUs gradually reduce when  $P_0$  decreases. This is because SUs have less opportunity to transmit when the PU occupies the channel more frequently.

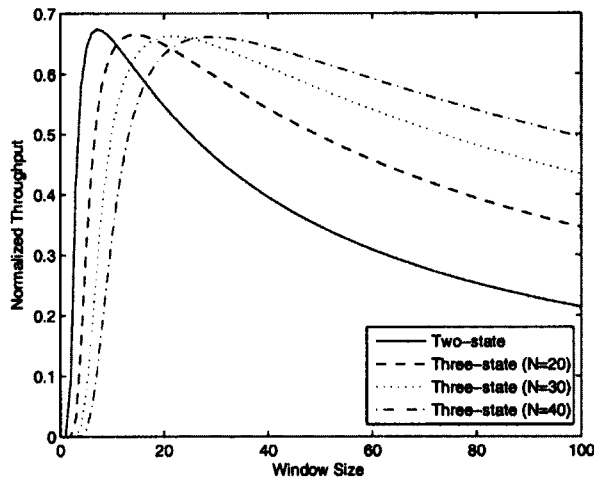


Fig. 15: Normalized throughput comparison between the two-state model and the three-state sensing model:  $P_0 = 0.8$

## V.4.2 FAIRNESS EVALUATION

The fairness performance is evaluated in the third experiment. Two scenarios with 5 and 10 co-existing CRNs are studied. For the sake of convenience, we assume each CRN contains one SU only. 20 cycles are observed from  $\Delta_1$  till  $\Delta_{20}$ . The period of  $\Delta_1$  equals the time to transmit 5 frames. Under the three-state sensing model, all SUs contend for the channel with the equal access probability  $P_a$ . Under the two-state model, we suppose each SU has 5 successive frames to transmit once it grasps the channel. Fig. 18 shows the Jain Index results with both models for 5 and 10 SUs.

It can be seen that the fairness of the three-state sensing model is dramatically improved compared to its peers. Especially, it is noticeable that fairness with differentiation is achieved fairly well even in a short period. This conclusion applies to both situations with 5 and 10 SUs. Let us next explore the influence of the number of SUs on the fairness performance. When the number of SUs increases from 5 to 10, the fairness of the



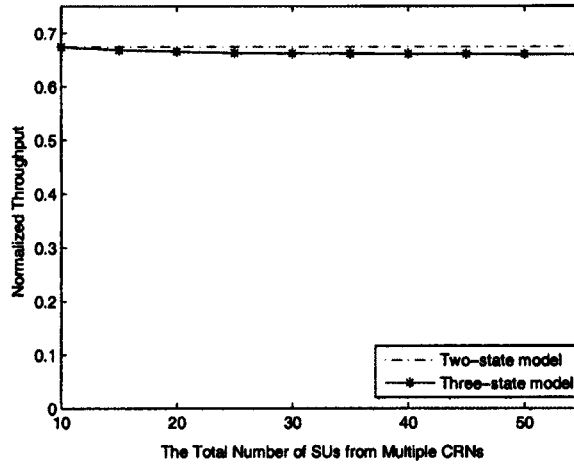


Fig. 16: Saturation throughput comparison between the two-state model and the three-state sensing model:  $P_0 = 0.8$

two-state model is dropped drastically. This suggests that the number of CRNs have significant impact on fairness and that fewer CRNs achieves better fairness. Nevertheless, in the three-state sensing model, the fairness has been slightly affected by the number of CRNs.

ALFA is further evaluated in the above four cases and the results are demonstrated in Fig. 19. This matches the conclusion drawn in Fig. 18. Concretely, the fairness from micro to macro level, in the three-state sensing model, is obtained satisfactorily (0.9103 for 5 SUs and 0.8707 for 10 SUs). The number of SUs does not greatly influence. In contrast, ALFA is far lower in the two-state model, with 0.6598 for 5 SUs and 0.4933 for 10 SUs.

## V.5 SUMMARY

In this chapter, multiple CRNs co-existing in an area have been considered. Accordingly, a three-state sensing model consisting of idle, occupied by a PU and occupied by an SU, is proposed. Based on this novel model, a fairness-achieved MAC (FMAC) has been designed that fully takes the PU activity into account. A Markov chain model tailored to the

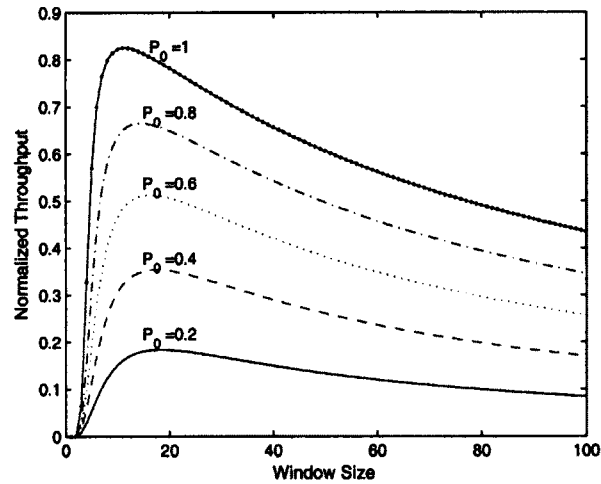


Fig. 17: The normalized throughput influenced by the PU activity

proposed FMAC has been derived. In addition, the performance of throughput and fairness of the three-state sensing model has been thoroughly examined. The numerical results have verified that the fairness of the three-state sensing model is significantly improved, while maintaining nearly the same throughput, in comparison to the two-state model.

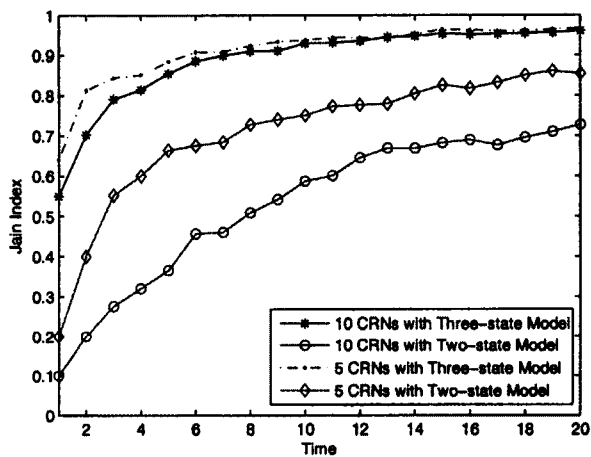


Fig. 18: Jain Index from  $\Delta_1$  to  $\Delta_{20}$

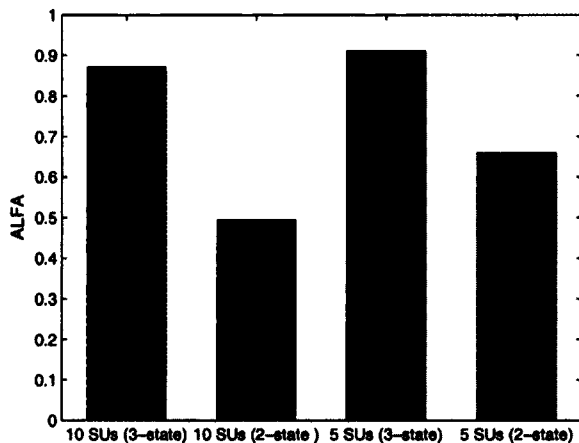


Fig. 19: ALFA comparison for 5 and 10 SUs with the two-state and three-state models

## CHAPTER VI

### DELAY ANALYSIS FOR CRNS SUPPORTING HETEROGENEOUS TRAFFIC

In Chapter V, two significant performance metrics of throughput and fairness have been carefully studied. Besides throughput and fairness, traffic delay is another critical network performance metric and has received very limited attention in CRNs. This chapter will study the delay analysis in a CRN supporting heterogeneous traffic. In general, traffic delay is defined as the period it takes for a packet to travel from a source to a destination, and can be divided into several components: the processing delay, queueing delay, transmission delay and propagation delay. The processing delay, transmission delay, and propagation delay can be straightforwardly determined for the given node processing power, network card speed, and nodes distance. On the contrary, queueing delay is a complicated quantity that depends on traffic load and various network states.

In this chapter, queueing delay for a CRN supporting heterogeneous service is the primary concern. In a multi-channel scenario, a channel selection scheme is designed, with the objective to reduce the average delay of all SU packets. In particular, the delay of an SU packet is affected not only by earlier SU packets in the queue, but also by the PU packets arriving during its waiting time. To address this issue, a virtual queue with different priorities is utilized to model the traffic of PUs and SUs on the same channel.

In order to guarantee PUs' licensed membership, packets from PUs are distinguished from SUs by employing an absolute priority scheme. Meanwhile, various delay requirements over the packets from SUs are fully considered. The packets from SUs are classified into either delay-sensitive packets or delay-insensitive packets. Moreover, a novel relative

priority strategy is designed between these two types of traffic by proposing a “transmission window” strategy. The delay performance of both a single-PU scenario and a multiple-PU scenario is thoroughly investigated employing queueing theory. In the multiple-PU scenario, a dynamic and adaptive channel selection scheme based on learning automata is developed with the objective of reducing the average delay for all SU packets. Numerical experiments are conducted and the results demonstrate the delay performance with respect to varied transmission window sizes. The results in the multiple-PU scenario verify that the proposed learning automata channel selection scheme significantly improves the delay performance of SU packets.

This chapter is organized as follows. Section VI.1 introduces the network model and main idea. Sections VI.2 and VI.3 present the detailed design of the channel selection algorithm as well as the delay performance along with an in-depth mathematical analysis. Numerical results are provided in Section VI.4. Summaries are concluded in Section VI.5.

## VI.1 NETWORK MODEL

A cognitive radio network consisting of  $M$  PUs and  $N$  SUs is considered, denoted as  $\mathbb{P}U = \{PU_1, PU_2, \dots, PU_m, \dots, PU_M\}$  and  $\mathbb{S}U = \{SU_1, SU_2, \dots, SU_n, \dots, SU_N\}$ . Let  $\mathbb{C} = \{C_1, C_2, \dots, C_m, \dots, C_M\}$  denote the set of channels. Heterogenous bandwidths of different channels is allowed, with the bandwidth of  $C_m$  denoted as  $B_m$ .

Due to the limitations of spectrum sensing, it is not feasible for an SU to detect all available channels. Furthermore, the available channels detected by different SUs may vary. Let  $\mathbb{C}_n$  denote the available channels detected by  $SU_n$ . Note that  $\mathbb{C}_n \subseteq \mathbb{C}$ . The ideal interference detection is assumed, i.e., an SU vacates the current channel immediately whenever

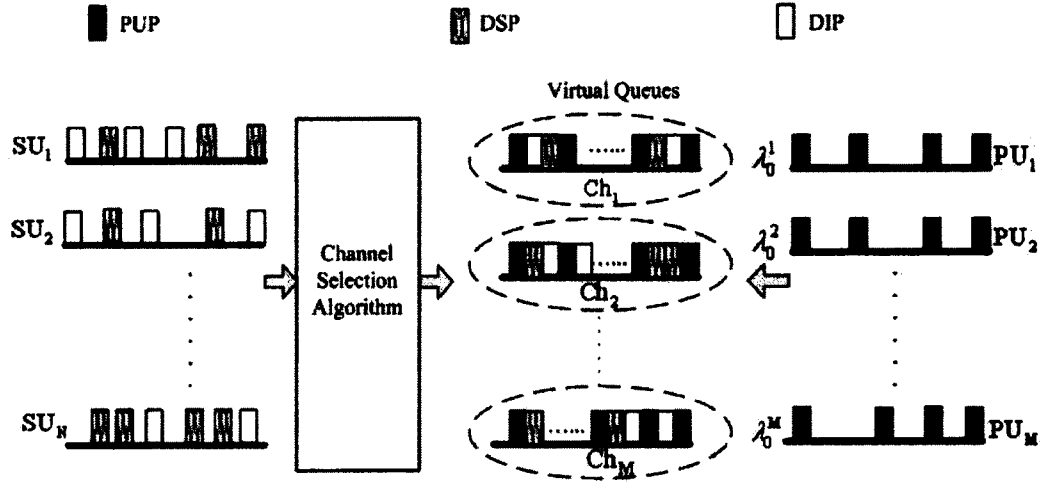


Fig. 20: Virtual queue model to process PU and SU packets

the corresponding PU reappears.

SUs are allowed to opportunistically access available channels when PUs are absent. An SU is assumed to occupy only one available channel to transmit data at a time. Each PU is assumed to occupy a dedicated channel and does not need to consider channel selection. However, an SU needs to select a channel prior to transmission. Let  $\mathbf{P}^n(k) = [p_1^n(k), p_2^n(k), \dots, p_M^n(k)]$  denote the access probability distribution of  $SU_n$  over  $M$  channels. The components of  $\mathbf{P}^n(k)$  satisfy  $\sum_{m=1}^M p_m^n(k) = 1$ . Based on its access probability distribution, each SU chooses a channel independently at the time slot  $k$ . Let  $x_m^n$  denote the channel selection result for the user  $SU_n$  choosing the channel  $C_m$  at the  $k^{\text{th}}$  time slot, where  $x_m^n(k) = 0$  or  $1$  and  $\sum_m x_m^n(k) = 1$ .

Heterogeneous services are supported in the considered network model. In general, heterogeneous services have different delay requirements. For instance, traffic delay has a significant impact on the quality of real-time data such as voice or video. In contrast, it has minor effect on time-insensitive services such as email. SU packets are divided into two broad categories in terms of delay requirement, namely the *delay-sensitive packets* (DSPs)

and *delay-insensitive packets* (DIPs). Each SU is assumed to generate both DSPs and DIPs. Our model can be easily extended to address more than two classes of SU packets. The priority levels of *PU packets* (PUPs), DSPs and DIPs are from high to low, denoted as level 0, 1 and 2.

In a cognitive radio network, SUs should be capable of correctly differentiating a PU signal from other SUs. PUPs from  $PU_m$  are assumed to follow Poisson distribution with rate  $\lambda_0^m$  using the channel  $C_m$ . Let  $\lambda_1^n, \lambda_2^n$  denote the average arrival rate of DSPs and DIPs from  $SU_n$ , which is modeled as a Poisson process. Let  $\mu_m^n$  denote the service rate for the  $n^{th}$  user using the channel  $C_m$ , which satisfies:

$$\mu_m^n = \frac{B_m}{L_n},$$

where  $L_n$  is the average packet size of the  $n^{th}$  user. This definition of  $\mu_m^n$  applies to both PUs and SUs. For a particular SU, note that its service rate under different channels may vary.

PUPs, DSPs and DIPs on the same channel are modeled as a virtual queue. Fig. 20 illustrates the whole picture of the system model.

## VI.2 SINGLE-PU SCENARIO

Before diving into the multiple-PU scenario, a scenario that consists of a single PU and a single SU is firstly considered.

### VI.2.1 TWO PRIORITY SCHEMES

PUPs have a strict priority over DSPs and DIPs. To prevent PUPs from disruption caused by DSPs and DIPs, an absolute priority scheme is employed for PUPs. In an absolute priority scheme, PUPs always access the channel whenever it appears. DSPs and DIPs

access the channel only if there are no PUPs. It is not appropriate to use an absolute priority scheme between DSPs and DIP, as the lower priority class may starve since the high priority class may seize the channel for a long time.

To avoid starvation of DIPs, a relative priority scheme is developed between DSPs and DIPs. Specifically, the incoming DSPs and DIPs are inserted into the same queue in the arrival order. A parameter  $W$  is introduced for the relative priority scheme. When the channel is available for SU traffic, the queue is searched from head to tail to find  $W$  DSPs (assuming that there are at least  $W$  DSPs in the queue). These  $W$  DSPs are labeled from 1 to  $W$ , in order of arrival. All packets that arrive earlier than the  $W^{th}$  DSP in the queue, including both DSPs and DIPs, form a *transmission window* (TW). Packets inside the TW are transmitted on the channel as follows. First, those  $W$  DSPs are transmitted in order of their arrival. After all  $W$  DSPs have been transmitted, DIPs in the current TW are transmitted, again, in arrival order. In case there are fewer than  $W$  DSPs in the queue, let  $L$  ( $L < W$ ) denote the number of DSPs in the queue. Packets are then transmitted on the channel as follows. The  $L$  DSPs are transmitted first, followed by the transmission of DIPs, if any. During the transmission period, newly arriving DSPs are inserted sequentially after the existing  $L$  DSPs. The current TW ends when the  $(W - L)^{th}$  newly arriving DSP has arrived. The above procedure is repeated until all packets in the current TW have been transmitted. Note that the size of TW may vary each time even with the same value of  $W$ . This depends on how many DIPs arrive in the TW. In the relative priority scheme, the higher the value of  $W$ , the higher the priority for DSPs is. Hence, by adjusting the parameter  $W$ , different priority levels between DSPs and DIPs can be achieved.

A relative priority scheme with  $W = 6$  is illustrated in Fig. 21, where clear rectangles



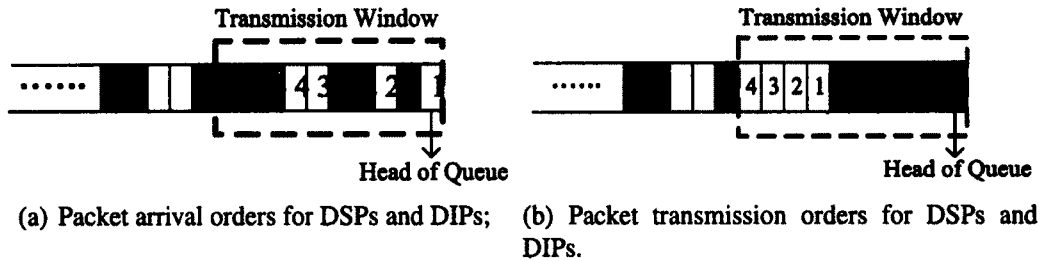


Fig. 21: Relative priority mechanism between DSPs and DIPs ( $W=6$ )

represent DIPs and shaded rectangles represent DSPs. Fig. 21(a) shows their arrival order of DSPs and DIPs. The TW based on  $W = 6$  is marked by the dotted line. The transmission order of DSPs and DIPs in the TW is described in Fig. 21(b).

## VI.2.2 DELAY ANALYSIS IN SINGLE-PU SCENARIO

In this section, the delay performance of PUPs, DSPs and DIPs is analyzed. Assume all the packets have equal size. Let the service time of a packet be a random variable  $S$ . As the delay of PUPs is not affected by DSPs and DIPs, it can be analyzed as an M/D/1 queue. Specifically, the delay of a PUP consists of two components: 1) the remaining service time of the current PUP (denoted by  $T_0^r$ ) in service, if any; 2) the time to serve all other PUPs (denoted by  $T_0^p$ ) that are waiting in the queue upon the arrival of this PUP. As a result, the mean queueing delay for a PUP, denoted by  $E[D_0]$ , can be represented as:

$$\begin{aligned}
 E[D_0] &= E[T_0^r] + E[T_0^p] \\
 \Rightarrow E[D_0] &= \frac{\rho_0}{2(1-\rho_0)\mu}, \tag{64}
 \end{aligned}$$

where  $\rho_0 = \lambda_0/\mu$ . Note that the superscripts of the notations is omitted in the single-PU scenario.

It is challenging to analyze the delay of DSPs and DIPs due to two issues. First, SUs

have to vacate the channel whenever the corresponding PU reappear. Second, with the relative priority scheme between DSPs and DIPs, although DSPs have a higher priority than DIPs in the same TW, DSPs have a lower priority than the DIPs in previous TWs. Both issues in the following delay analysis of DSPs and DIPs will be addressed.

The queueing delay for a DSP, denoted as  $D_1$ , consists of four components: 1) the remaining service time of the current packet, either a PUP or a DSP, in service, if any; 2) the time to serve all other PUPs and DSPs that are waiting in the queue upon the arrival of this DSP; 3) the time to serve the PUPs that arrive during the queueing time of this DSP; 4) the time to serve all the DIPs in previous TWs if there is at least one TW in the queue when this DSP arrives. Note that for a DSP falling into the  $(\alpha + 1)^{th}$  TW ( $\alpha = 1, \dots, \infty$ ) in the queue, all DIPs in the previous  $\alpha$  TWs should be served before this DSP.

The first two components can be obtained using the approach in [54] as  $E[T_0^r] + E[T_1^r]$ . The third component can be represented as  $\rho_0 E[D_1]$ . The fourth component is calculated in the following. The probability that a DSP falling into the  $(\alpha + 1) \cdot W$  DSPs can be expressed as:

$$\begin{aligned} P^* &= \Pr[\alpha W \leq \text{number of DSP packets} < (\alpha + 1)W] \\ &= \rho_1^{\alpha W} - \rho_1^{(\alpha+1)W-1} = \rho_1^{\alpha W} (1 - \rho_1^{(W-1)}), \end{aligned} \quad (65)$$

where  $\rho_1 = \lambda_1 / \mu$ .

There are  $W$  DSPs inside each TW. Because both DSPs and DIPs follow Poisson arrival with rate  $\lambda_1$  and  $\lambda_2$ , respectively, the mean number of DIPs in  $\alpha$  TWs is  $\alpha \cdot W \cdot \frac{\lambda_2}{\lambda_1}$ . Thus, the mean time to serve DIPs in previous TWs in the queue when a DSP arrives can be derived

as:

$$\begin{aligned}
& \sum_{\alpha=1}^{\infty} \rho_1^{\alpha W} (1 - \rho_1^{(W-1)}) \cdot \frac{\alpha W \lambda_2}{\mu \lambda_1} \quad (66) \\
&= \frac{\lambda_2 \rho_1 (1 - \rho_1^{(W-1)})}{\mu \lambda_1} \frac{d \left( \sum_{\alpha=1}^{\infty} \rho_1^{\alpha W} \right)}{d \rho_1} \\
&= \frac{\rho_2 W \rho_1^W (1 - \rho_1^{(W-1)})}{\lambda_1 (1 - \rho_1^W)^2} \\
&\approx \frac{\rho_2 W \rho_1^W}{\lambda_1 (1 - \rho_1^W)},
\end{aligned}$$

where  $\rho_2 = \lambda_2 / \mu$ .

Combining all four components of DSP queueing delay, the mean delay of a DSP,  $E[D_1]$  can be expressed as:

$$\begin{aligned}
E[D_1] &= \sum_{i=0}^1 E[T_i^r] + \sum_{i=0}^1 E[T_i^p] \\
&\quad + \rho_0 E[D_1] + \frac{\rho_2 W \rho_1^W}{\lambda_1 (1 - \rho_1^W)} \\
&= \frac{1}{2} \sum_{i=0}^1 \lambda_i E[S_i^2] + \sum_{i=0}^1 \rho_i E[D_i] \\
&\quad + \rho_0 E[D_1] + \frac{\rho_2 W \rho_1^W}{\lambda_1 (1 - \rho_1^W)} \\
\Rightarrow E[D_1] &= \frac{\lambda_0 + (1 - \rho_0) \lambda_1}{2(1 - \rho_0)(1 - \rho_0 - \rho_1) \mu^2} \\
&\quad + \frac{\rho_2 W \rho_1^W}{\lambda_1 (1 - \rho_1^W)(1 - \rho_0 - \rho_1)}, \quad (67)
\end{aligned}$$

Eq. (67) indicates that parameter  $W$  plays a significant role in the queueing delay of DSPs. This will be verified in Section VI.4.

Next, the analysis for the queueing delay of DIPs is carried out. For an incoming DIP, the queueing delay, denoted as  $D_2$ , consists of four components: 1) the remaining service time of a PUP, DSP, or DIP, in service, if any; 2) the time to serve all other PUPs, DSPs,

and DIPs that are in the queue upon the arrival of this DIP; 3) the time to serve PUPs that arrive during the queueing time of this DIP; 4) the time to serve DSPs in the same TW that arrive during queueing time of this DIP.

The first three components can be obtained as similarly to those in Eq. (67). The fourth component is examined next. Note that although there are  $W$  DSPs in each TW, some of these  $W$  DSPs may have arrived after this DIP leaves the queue and proceeds to the destination. Certainly these DSPs cannot be served before this DIP. Furthermore, there may be some DSPs that arrive during queueing time of this DIP, but belong to the future TWs (after the current TW). These DSPs should not be served before this DIP. Let  $V$  denote the number of DSPs that are in the same TW of this DIP and have arrived before this DIP. Let  $U$  denote the number of DSPs that arrive during queueing time of this DIP. Then the fourth component, defined as  $Z$ , is the time to serve  $E(\min\{W - V, U\})$  number of DSPs. Unfortunately, it is intractable to directly derive  $Z$ . Instead, the lower and upper bounds for this quantity is derived. Considering that the  $W$  DSPs in a TW are  $W$  points and there is one position before each point, then, due to the Poisson arrival, a DIP has the same probability to arrive at any of the  $W$  positions. Therefore, in the current TW, there are at most  $W$  DSPs arriving during the queueing time of this DIP. On the other hand, there may be no DSP arriving, e.g., the DSP following this DIP takes too long to arrive. Then  $0 \leq Z \leq W/\mu$  holds. As a result, the approximate mean  $E(Z) \approx \frac{W}{2\mu}$  is obtained. Based on above discussions, the

mean delay,  $E[D_2]$ , can be expressed as:

$$\begin{aligned}
E[D_2] &= \sum_{i=0}^2 E[T_i^r] + \sum_{i=0}^2 E[T_i^p] + \rho_0 E[D_2] + E(Z) \\
&= \frac{1}{2} \sum_{i=0}^2 \lambda_i E[S_i^2] + \sum_{i=0}^2 \rho_i E[D_i] + \rho_0 E[D_2] + E(Z) \\
\Rightarrow E[D_2] &= \frac{\frac{1}{2\mu^2} \sum_{i=0}^2 \lambda_i + \sum_{i=0}^1 \rho_i E[D_i] + \frac{W}{2\mu}}{(1 - \rho_0 - \rho_2)} \tag{68}
\end{aligned}$$

### VI.3 MULTIPLE-PU SCENARIO

#### VI.3.1 DYNAMIC CHANNEL SELECTION ALGORITHM

In the multiple-PU scenario, each SU needs to select a proper available channel prior to transmission. Since there can be multiple available PU channels for SUs, a dynamic and decentralized channel selection scheme based on LA is developed in this section. Each SU implements the channel selection algorithm locally. Let  $\mathbf{P}^n(k) = [p_1^n(k), p_2^n(k), \dots, p_M^n(k)]$  denotes the access probability distribution of  $SU_n$  over  $M$  channels. Let  $\mathbf{X}^n(k) = [x_1^n(k), x_2^n(k), \dots, x_M^n(k)]$  denote the channel selection vector for the user  $SU_n$  at the  $k^{\text{th}}$  time slot. Each SU receives a payoff in response to the chosen channel. Let  $\beta_m^n(k)$  denote the payoff for the  $SU_n$  to choose the channel  $C_m$ . Our objective for channel selection is to decrease the queuing delay for SU traffic. In Eqs. (67) and (68), the queuing delay decreases when the service rate increases. All packets are assumed to have the same size and hence the service rate on channel  $C_m$  is the same for each packet, which is denoted as  $\mu_m$ . Hence  $\beta_m^n(k)$  should be proportional to  $\mu_m$ . Moreover, for an arriving SU packet, the existing SU packets in the queue impact the delay of this arriving packet. Specifically, if the arriving packet is a DSP, all existing DSPs and some DIPs affect its delay. On the other

hand, if the incoming packet is a DIP, all existing DSPs and DIPs are taken into account for the delay. To differentiate these two cases, a weight  $\theta(0 < \theta \leq 1)$  is introduced. Based on the above discussion,  $\beta_m^n(k)$  is designed as follows:

$$\beta_m^n(k) = \frac{\mu_m}{\sum_{j=1}^N (x_m^j \cdot \lambda_1^j) + \theta \cdot \sum_{j=1}^N (x_m^j \cdot \lambda_2^j)} \quad (69)$$

where  $0 < \theta < 1$  when  $SU_n$  generates DSP and  $\theta = 1$  when  $SU_n$  generates DIP.

By recording all previous chosen channels and the corresponding payoffs, the reward probability can be computed as  $d_m^n(k) = \frac{B_m^n(k)}{Z_m^n(k)}$ , where  $Z_m^n(k)$  is the number of time slots that the  $SU_n$  chooses the channel  $C_m$ , until the time slot  $k$ .  $B_m^n(k)$  is the sum of  $\beta_m^n$  in these time slots. The optimal channel is believed to be  $i = \arg \max_m \{d_m^n\}$ . Then the access probability  $\mathbf{P}^n(k)$  is updated to  $\mathbf{P}^n(k+1)$  as follows:

$$\mathbf{P}^n(k+1) = \mathbf{P}^n(k) + \gamma[\mathbf{e}_i - \mathbf{P}^n(k)], \quad (70)$$

where  $\gamma(0 \leq \gamma \leq 1)$  is a step-size parameter and  $\mathbf{e}_i$  is the identity vector with the  $i^{\text{th}}$  element 1 and all others 0.

The channel selection algorithm for  $SU_n$  is described in **Algorithm 3**, which is a learning automata (LA) based algorithm. The advantage of LA is that it can converge to an  $\epsilon$ -optimal solution reasonably quickly [41]. This means that **Algorithm 3** is feasible and a stable access probability will eventually be obtained. Specifically, at time slot  $k$ , the channel selection vector  $\mathbf{X}^n(k)$  for the user  $SU_n$  is obtained based on the channel access probability  $\mathbf{P}^n(k)$ . During the first few time slots, the chosen channels might be different for a particular SU. Nevertheless, after some startup time, each SU will choose a fixed

channel for a relatively long time. That will be verified in Section VI.4.

### VI.3.2 DELAY ANALYSIS IN MULTIPLE-PU SCENARIO

Let  $E[D_0^m]$  denote the mean delay for the packets of the user  $PU_m$ . Since the PU packets are not affected by the SU packets under the absolute priority scheme, and each PU has a dedicated channel,  $E[D_0^m]$  is obtained the same as the  $E[D_0]$  in the single-PU scenario. Hence, from Eq. (64),  $E[D_0^m]$  is given as:

$$E[D_0^m] = \frac{\rho_0^m}{2(1 - \rho_0^m)\mu_m}, \quad (71)$$

where  $\rho_0^m = \lambda_0^m / \mu_m$ .

Next, the delay of DSPs and DIPs is analyzed. After **Algorithm 3** terminates, SUs on channel  $C_m$  are statistically stable thanks to the convergence property of LA. The SUs on the same channel are treated as a group, and time synchronization is performed among them. Then, SUs can use a collision free MAC scheme, e.g., a collision-free TDMA scheme. This can be achieved by employing a base station in the network. Note that the scheduling process may introduce additional delay, which is ignored in this chapter.

In the multiple-PU scenario, the same priority scheme as in the single-PU scenario is employed among PUPs, DSPs, and DIPs. Namely, the absolute priority is adopted for PUPs against DSPs and DIPs, and the relative priority is used between DSPs and DIPs. Similarly, the TW strategy in the single-PU scenario is also utilized for the multiple-PU scenario. Specifically, the incoming DSPs and DIPs from all SUs that select the same channel are 'labeled' based on their arrival orders. The PUPs from  $PU_m$ , and the DSPs and DIPs from the SUs selecting channel  $C_m$  are processed by one virtual queue.

The mean delay for a DSP on channel  $C_m$  is denoted by  $E[D_1^m]$ .  $E[D_1^m]$  consists of four

components similar to  $E[D_1]$  in the single-PU scenario. The major difference is that the rate of incoming DSP traffic changes from  $\lambda_1$  to  $\sum_{n=1}^N (x_m^n \cdot \lambda_1^n)$ , denoted by  $\widetilde{\lambda}_1^m$ . Similarly, the rate of incoming DIP traffic changes from  $\lambda_2$  to  $\sum_{n=1}^N (x_m^n \cdot \lambda_2^n)$ , denoted by  $\widetilde{\lambda}_2^m$ . Accordingly,  $E[D_1^m]$  can be written as

$$\begin{aligned}
 E[D_1^m] &= \frac{1}{2} \sum_{i=0}^1 \overline{\lambda}_i^m E[S_i^2] + \rho_0^m E[D_0^m] + \frac{\widetilde{\lambda}_1^m}{\mu_m} E[D_1^m] \\
 &\quad + \rho_0^m E[D_1^m] + \frac{W \widetilde{\lambda}_2^m \left(\frac{\widetilde{\lambda}_2^m}{\mu_m}\right)^W}{\mu_m \overline{\lambda}_1^m \left[1 - \left(\frac{\widetilde{\lambda}_1^m}{\mu_m}\right)^W\right]}
 \end{aligned} \tag{72}$$

$$\begin{aligned}
 \Rightarrow E[D_1^m] &= \frac{\lambda_0^m + (1 - \rho_0^m) \overline{\lambda}_1^m}{2(\mu_m)^2 \left(1 - \rho_0^m - \frac{\widetilde{\lambda}_1^m}{\mu_m}\right) (1 - \rho_0^m)} \\
 &\quad + \frac{W \widetilde{\lambda}_2^m \left(\frac{\widetilde{\lambda}_1^m}{\mu_m}\right)^W}{\mu_m \overline{\lambda}_1^m \left[1 - \left(\frac{\widetilde{\lambda}_1^m}{\mu_m}\right)^W\right] (1 - \rho_0^m - \frac{\widetilde{\lambda}_1^m}{\mu_m})},
 \end{aligned}$$

where  $\overline{\lambda}_i^m = \frac{\widetilde{\lambda}_i^m}{\sum_{n=1}^N x_m^n}$ . Continuingly, the average delay of DSPs in the entire system, denoted by  $E[D_1]$ , can be computed as follows:

$$E[D_1] = \frac{1}{M} \sum_{m=1}^M E[D_1^m]. \tag{73}$$

The mean delay for a DIP on the channel  $C_m$  is denoted as  $E[D_2^m]$ . The rate of incoming DSP and DIP traffic are  $\widetilde{\lambda}_1^m$  and  $\widetilde{\lambda}_2^m$ , respectively. Similar to  $E[D_2]$  in the single-PU scenario,



$E[D_2^m]$  contains four components and can be derived as:

$$\begin{aligned}
E[D_2^m] &= \frac{1}{2} \sum_{i=0}^1 \bar{\lambda}_i^m E[S_i^2] + \rho_0^m E[D_0^m] \\
&\quad + \sum_{i=1}^2 \left( \frac{\tilde{\lambda}_1^m}{\mu_m} \right) E[D_i^m] + \rho_0^m E[D_2^m] \\
&\quad + E[Z^m] \\
\Rightarrow E[D_2^m] &= \frac{\frac{1}{2(\mu^m)^2} \sum_{i=0}^2 \bar{\lambda}_i^m + \rho_0^m E[D_0^m] + \left( \frac{\tilde{\lambda}_1^m}{\mu_m} \right) E[D_1^m] + \frac{W}{2\mu_m}}{(1 - \rho_0^m - \frac{\lambda_2^m}{\mu_m})}
\end{aligned}$$

Correspondingly, the average delay of DIPs in the entire system, denoted by  $E[D_2]$ , can be computed as follows:

$$E[D_2] = \frac{1}{M} \sum_{m=1}^M E[D_2^m]. \quad (74)$$

## VI.4 NUMERICAL RESULTS

### VI.4.1 SINGLE-PU SCENARIO

In the single-PU scenario, there is only one channel, shared by one PU and one SU. The channel bandwidth is assumed 1Mbps. The packet size is assumed as 512 bytes. In the first experiment, the Poisson arrival rates  $\lambda_0$ ,  $\lambda_1$ , and  $\lambda_2$  of PUP, DSP, and DIP traffic are assumed to be 100, 75, and 50 packets per second, respectively. In Fig. 22, the mean delay of PUPs, DSPs, and DIPs is plotted as a function of the TW size ( $W$ ). It can be seen that  $E[D_0]$  has a constant value when  $W$  changes. The  $E[D_1]$  decreases slightly, while  $E[D_2]$  increases dramatically, when  $W$  increases. As mentioned in Section VI.2, the TW size  $W$  is used to adjust the relative priority between DSPs and DIPs. The results in Fig. 22 confirm our design goal of using the relative priority between DSPs and DIPs.

In the second experiment, the TW size  $W$  is fixed as 5. The DSPs and DIPs arrival rates,

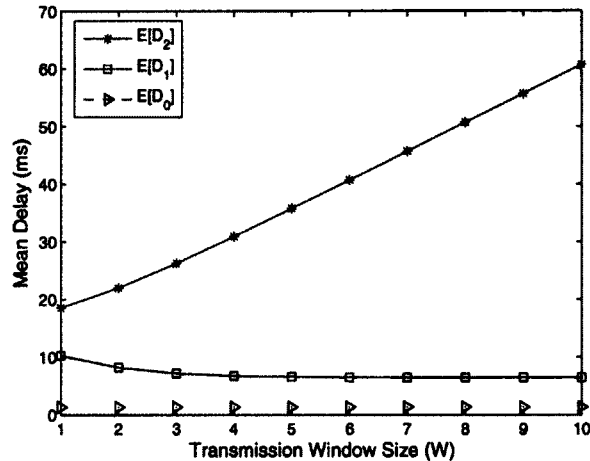


Fig. 22: Mean delays of PUPs, DSPs and DIPs in the single-PU scenario

$\lambda_1$  and  $\lambda_2$ , remain the same as in the first experiment, while the PUPs arrival rate  $\lambda_0$  varies. Fig. 23 shows the mean delay of PUPs, DSPs and DIPs as a function of  $\lambda_0$ . It can be seen that  $E[D_0]$ ,  $E[D_1]$ , and  $E[D_2]$  all increase when  $\lambda_0$  grows.  $E[D_2]$  has the most significant delay followed by  $E[D_1]$ .  $E[D_0]$  has the slightest increase. This can be explained as follows. When the arrival rate of PUPs increases, the channel occupancy by the PU becomes longer. This reduces the opportunity for DSPs to access the channel. Moreover, the DIPs have the lowest priority. When even DSPs have difficulty to access the channel, the chance is even worse for DIPs, and thus the delay increment for DIPs is the most significant.

#### VI.4.2 MULTIPLE-PU SCENARIO

The channel selection algorithm (LACS) is first examined. In this experiment, the number of PUs and SUs is assumed to be 5 and 10. The bandwidths of the five channels are set as 4.1353, 8.5600, 5.1785, 6.6997, and 4.1595 Mbps, following a uniform distribution between 3 and 10 Mbps. The arrival rates of PUPs, DSPs and DIPs  $\lambda_0^m$ ,  $\lambda_1^n$  and  $\lambda_2^n$ , are 100, 75, and 50 packets per second, respectively. For each SU, the channel selection probability

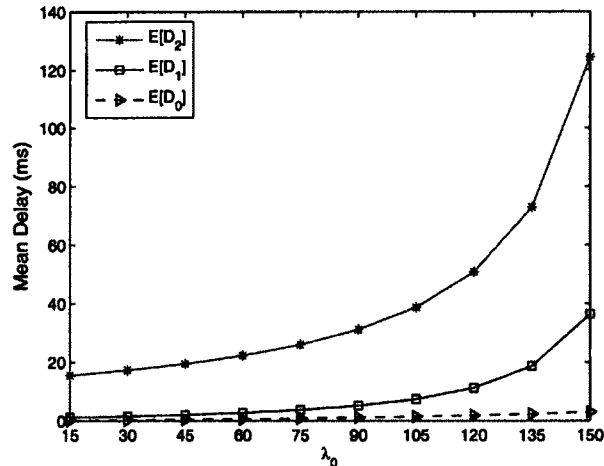


Fig. 23: Mean delays as a function of  $\lambda_0$  in the single-PU scenario

is updated dynamically at each time slot. Due to the limited space, only two SUs as examples are demonstrated, denoted as  $SU_1$  and  $SU_2$ , to examine the channel selection dynamics over time. Fig. 24 illustrates the channel selection probabilities of  $SU_1$  over time slots 1 to 10. The probability of selecting channel 2 quickly increases and approaches 1 at the 10<sup>th</sup> time slot. On the other hand, the probabilities of selecting other channels decreases over time and approach 0 at the 10<sup>th</sup> time slot. Hence the channel chosen for  $SU_1$  after some startup time should be channel 2. Fig. 25 shows the channel selection probabilities of  $SU_2$ . For  $SU_2$ , the probability of choosing channel 3 steadily increases and approaches 1. This implies that  $SU_2$  will finally select channel 3 after some startup time. There is a similar observation for all other SUs, i.e., the chosen channel might vary from time slot to time slot at the beginning, but will finally settle down to a specific channel after the startup time. Such observations verify the convergence of our channel selection algorithm.

Now, the mean queueing delay will be evaluated. The queueing delay with our proposed channel selection algorithm (LACS) is compared with the one obtained using a *random*

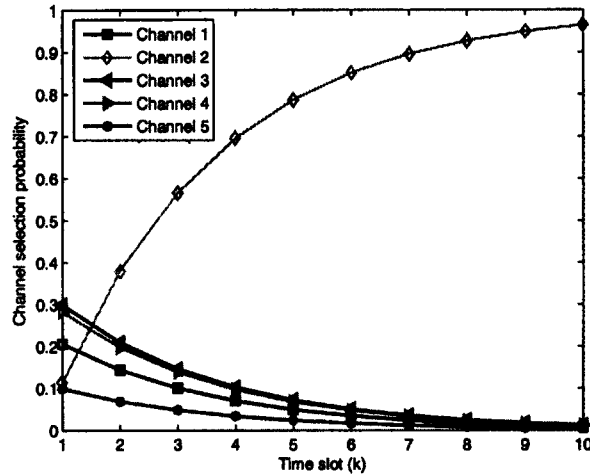


Fig. 24: Channel access probability for SU1

*channel selection* (RCS) algorithm [55]. Four experiments have been carried out, in which the channel bandwidths,  $\lambda_1^n$  and  $\lambda_2^n$ , remain the same as in the previous channel selection experiment. In the first experiment, 5 PUs and 10 SUs are assumed. Two values, 100 and 300 packets per second, are adopted respectively, for the arrival rate of PUPs,  $\lambda_0^m$ . The mean delays are plotted in Fig. 26. The delay of PUPs,  $E[D_0]$ , remains constant and is not affected by the channel selection algorithm, since the channel selection only applies to SUs. For the delay of DSPs and DIPs,  $E[D_1]$  and  $E[D_2]$ , the proposed LACS outperforms the RCS in both cases.

In the second experiment, 5 PUs and 20 SUs are assumed. The arrival rates of PUPs, DSPs, and DIPs are the same as in the first experiment. The mean delays are shown in Fig. 27. By comparing Fig. 27 and Fig. 26, it can be seen that the performance improvement of LACS compared with RCS is more significant when there are more SUs. This is because more SUs result in a higher traffic load, and the role of the channel selection algorithm becomes more critical under higher loads.

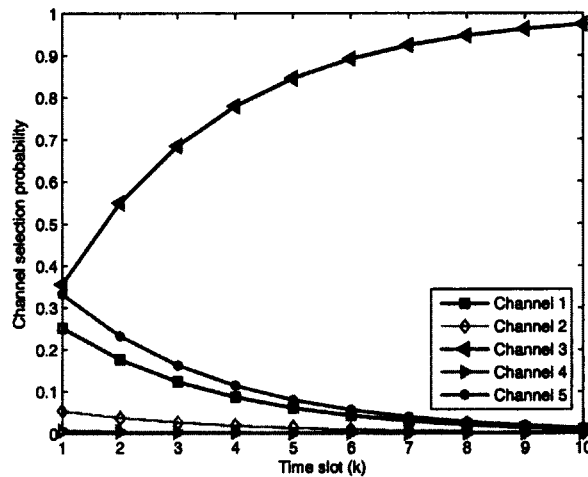


Fig. 25: Channel access probability for SU2

In the third experiment, the mean delay as a function of the PUPs arrival rate  $\lambda_0^m$  is examined, while fixing the TW size  $W$  as 5. The number of PUs and SUs, and the arrival rates of DSPs and DIPs remain the same as in the first experiment. Similar to Fig. 23, Fig. 28 shows that the mean delays of PUPs, DSPs, and DIPs all increase when  $\lambda_0^m$  increases. Specifically,  $E[D_2]$  grows faster than  $E[D_1]$  and  $E[D_0]$ . This confirms the effectiveness of the priority scheme used between PUPs, DSPs, and DIPs.

In the last experiment, the number of SUs is increased to 20 while maintaining other parameters as the same in the third experiment. The results depicted in Fig. 29 verify the observations from Fig. 28. That is, the mean delays of PUPs, DSPs and DIPs grow when  $\lambda_0^m$  increase. In addition, the mean delays under RCS grows faster compared with Fig. 28.

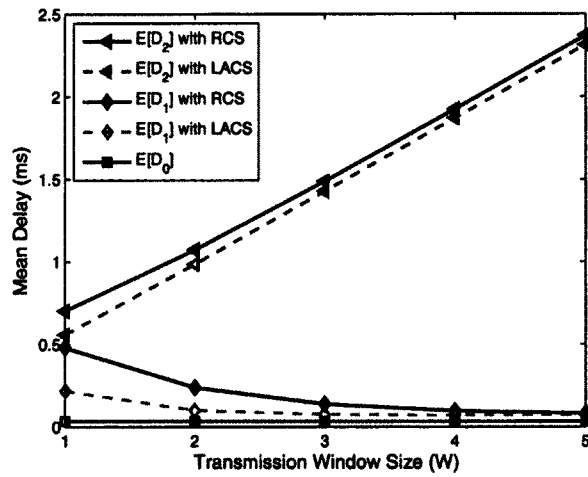
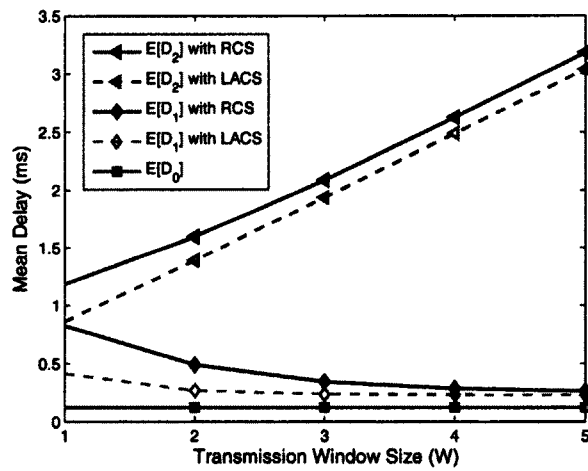
(a)  $\lambda_0^m = 100$ (b)  $\lambda_0^m = 300$ 

Fig. 26: Mean delays under LACS and RCS in the multiple-PU scenario, with 5 channels and 10 SUs

## VI.5 SUMMARY

In this chapter, the queuing delay of *PU packets* (PUPs), *delay-sensitive SU packets* (DSPs), and *delay-insensitive SU packets* (DIPs) in both single-PU and multiple-PU scenarios are analyzed. A relative priority scheme has been proposed using the *transmission*

*window* technology to differentiate DSPs and DIPs. Furthermore, in the multiple-PU scenario, a channel selection algorithm based on *learning automata* (LA) has been designed, with the objective to reduce the queueing delay. The numerical results show that the priority scheme is effective in differentiating the delays of PUPs, DSPs, and DIPs, and the proposed channel selection algorithm improves the queueing delay significantly.

---

**Algorithm 3** Learning automata based channel selection (LACS) algorithm
 

---

- 1: Initialization:  $k = 0, \gamma = 0.5, B_m^n(0) = Z_m^n(0) = 0$ .
  - 2: Assign the initial channel access probability randomly with a constraint:  

$$\sum_{m \in C_n(k)} p_m^n(0) = 1$$
  - 3: Pick a channel according to  $p_m^n(k)$ :  $p_m^n(k) \Rightarrow X_m^n(k)$ .
  - 4: **for**  $m=1:1:M$  **do**
  - 5:   **if** the  $m^{th}$  channel is chosen **then**
  - 6:      $Z_m^n(k) = Z_m^n(k) + 1$ ;
  - 7:      $B_m^n(k) = B_m^n(k) + \beta_m^n(k)$ ;
  - 8:      $d_m^n(k) = \frac{B_m^n(k)}{Z_m^n(k)}$ ;
  - 9:   **end if**
  - 10: **end for**
  - 11: Search for the maximum  $d_m^n(k)$ :  $i = \arg \max_m \{d_m^n(k)\}$
  - 12: Update the channel access probability:
  - 13: **for**  $m = 1 : 1 : M$  **do**
  - 14:   **if**  $m=i$  **then**
  - 15:      $p_i^n(k+1) = p_i^n(k) + \gamma[1 - p_i^n(k)]$ ;
  - 16:   **else**
  - 17:      $p_m^n(k+1) = p_m^n(k) - \gamma p_m^n(k)$ ;
  - 18:   **end if**
  - 19: **end for**
  - 20: **if**  $p^n(k)$  contains an element  $1 - \varepsilon$  ( $0 < \varepsilon \ll 1$ ) at the  $j^{th}$  channel **then**
  - 21:   **if**  $m=j$  **then**
  - 22:      $x_j^n(k) = 1$
  - 23:   **else**
  - 24:      $x_m^n(k) = 0$
  - 25:   **end if**
  - 26:   **STOP**
  - 27: **else**
  - 28:    $k = k + 1$ ;
  - 29:   **GOTO** Line 3
  - 30: **end if**
-



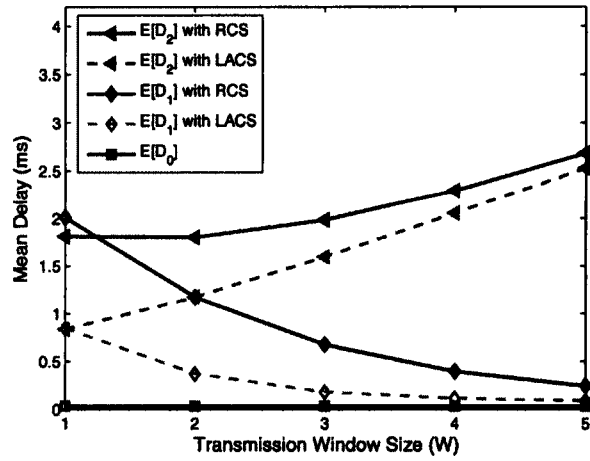
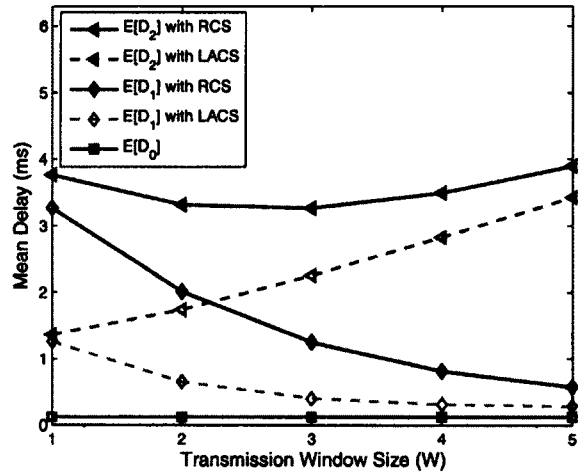
(a)  $\lambda_0^m = 100$ (b)  $\lambda_0^m = 300$ 

Fig. 27: Mean delays under LACS and RCS in the multiple-PU scenario, with 5 channels and 20 SUs.

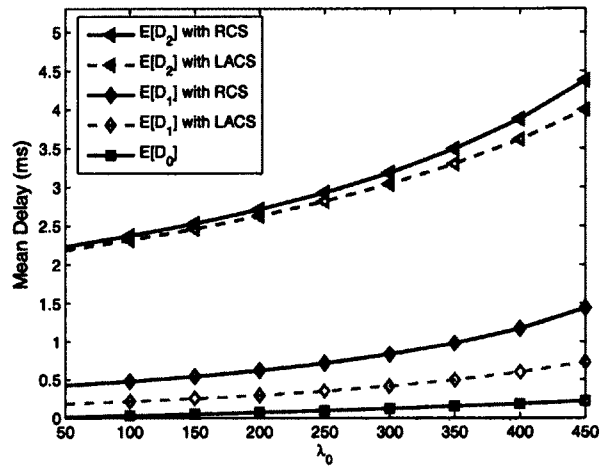


Fig. 28: Mean delays in the multiple-PU scenario, as a function of  $\lambda_0^m$ , with 5 channels and 10 SUs

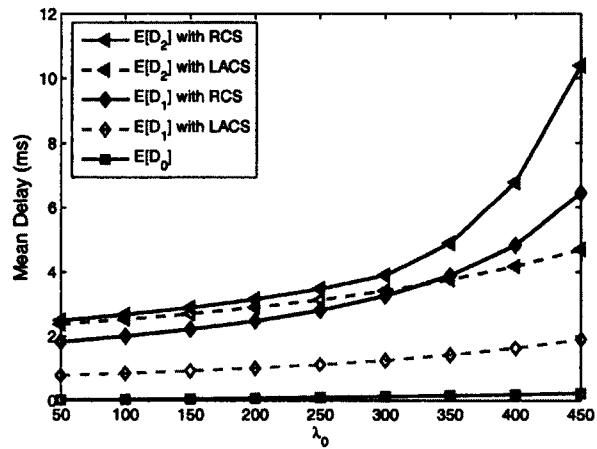


Fig. 29: Mean delays in the multiple-PU scenario, as a function of  $\lambda_0^m$ , with 5 channels and 20 SUs

## CHAPTER VII

### CONCLUSIONS AND FUTURE RESEARCH

The preceding chapters have studied several crucial aspects of spectrum sensing, throughput, fairness and delay analysis in CRNs. This chapter will summarize the major contributions in section VII.1 and shed light on directions for further research in section VII.2.

#### VII.1 CONCLUSIONS

The main contributions presented in this dissertation are listed below:

- A weighted cooperative spectrum sensing framework for infrastructure-based cognitive radio networks has been designed. The framework consists of two modules. In the first module, each SU conducts local spectrum sensing and computes the total error probability. The total error probability and the energy signal from the PU are then sent to the base station. In the second module, the base station makes a final decision through combining the weighted energy signals from all SUs. To reduce the computation complexity and communication overhead, not all SUs report their local sensing results to the base station. The minimum number of SUs required to participate in cooperative sensing has been derived. Numerical results have verified that the proposed weighted cooperative spectrum sensing framework significantly improves the sensing accuracy.
- Co-existing multiple CRNs in one area have been thoroughly studied, which have

received little attention. Accordingly, a smart three-state sensing model has been proposed, which distinguishes the channel as *idle*, *occupied by a PU*, or *occupied by an SU*. To accurately detect each state of the three, a methodology of a two-stage detection procedure has been developed. In the first stage, energy detection is employed to identify whether a channel is idle or occupied. If the channel is occupied, the received signal is further analyzed at the second stage, aiming at determining whether the signal originates from a PU or an SU. At the second stage, a statistical model is developed, which is used for distance estimation. With regard to detection performance, the false alarm and miss detection probabilities for the proposed spectrum sensing technology have been theoretically analyzed in both local and cooperative sensing scenarios.

- The performance analysis of the smart sensing model has been deeply investigated. A *fairness-achieved media access control (FMAC)* protocol has been developed. Associated with the FMAC, a novel two-tier Markov chain model is created, which fully considers the PU activity. Two significant performance metrics, namely throughput and fairness, have been carefully studied. In terms of fairness, the fairness dynamics from a micro-level to macro-level is evaluated among SUs from multiple CRNs. Also, the fundamental distinctions between the two-state model and the three-state sensing model have been addressed.
- The delay performance of a CRN supporting heterogeneous traffic has been examined, in which priority differentiation for SU packets is taken into account. The packets are classified into three classes, PUPs, DSPs and DIPs. The priority levels

of PUPs, DSPs and DIPs are denoted as 0, 1, 2, from high to low. Furthermore, an absolute priority scheme is employed for PUPs to guarantee their licensed privilege. To avoid the starvation of the lowest priority traffic, instead, a relative priority strategy is designed between DSPs and DIPs, using a “transmission window” strategy. In the multiple-PU scenario, a dynamic and adaptive channel selection strategy based on learning automata is developed. It aims to reduce the average delay of SU packets. Afterwards, the transmission of PUPs, DSPs and DIPs on the same channel are modeled as a virtual queue with three different priorities. Queueing delay is analyzed in both the single-PU and multiple-PU scenarios. The numerical results have shown that the priority scheme is effective in differentiating the delays of PUPs, DSPs, and DIPs, and the proposed channel selection algorithm have improved the queueing delay significantly.

## VII.2 FUTURE RESEARCH

In this section, the future research will be discussed. There are a number of ways to extend current research. The following lists some possible directions for the future directions.

- In the spectrum sensing presented in Chapter III.1, the PU signal level is assumed relatively higher than noise. However, this does not hold in certain cases. As we know, severe noise is an important factor in the degradation of the detection accuracy. The inherent uncertainty of noise makes the differentiation between signal and noise very challenging. Authors in [56] conclude that there exists an “SNR Wall” for matched filter detection, energy detection and feature detection. Below a specific “SNR Wall”, these three detectors will fail to differentiate noise from signals, no matter how long

the detector can observe the channel. To meet the strict requirements of the *Federal Communications Commission* (FCC), novel methods are needed to be designed which are efficient and robust to noise.

- Reliability is one of the most significant performance metrics in wireless applications. Unfortunately, malicious users always exist and destroy normal user's services. Taking cognitive radio networks as an instance, malicious SUs may falsely report their detection result, or even worse, they imitate the behavior of primary users. This will lead to poor detection accuracy and thus degrade the benefits of normal SUs. So one possible direction is to extend current spectrum sensing technology while taking the security issue into account.
- Most of the current literature is limited to the theoretical analysis, in which a couple of strong assumptions are usually taken for granted. For instance, one fundamental assumption is that noise follows Additive White Gaussian Noise (AWGN), which is also used in this dissertation. In fact, noise in an actual wireless environment is far more complicated. To be more practical, large-scale experimental implementations are needed to provide scientific benchmarks for aforementioned issues. Both positive and negative results from implementations are valuable to reflect insights back into the theoretical studies.

## REFERENCES

- [1] S. Haykin, "Cognitive radio: brain-empowered wireless communications," *IEEE Journal on Selected Areas in Communications*, vol. 23, no. 2, pp. 201–220, 2005.
- [2] S. Force, "Spectrum policy task force report," *Federal Communications Commission ET Docket 02*, vol. 135, 2002.
- [3] G. Ganesan and Y. Li, "Agility improvement through cooperative diversity in cognitive radio," in *Proc. IEEE Global Telecommunications Conference (GLOBECOM)*, vol. 5, pp. 2505–2509, 2005.
- [4] M. Gandetto and C. Regazzoni, "Spectrum sensing: A distributed approach for cognitive terminals," *IEEE Journal on Selected Areas in Communications*, vol. 25, no. 3, pp. 546–557, 2007.
- [5] Z. Quan, S. Cui, and A. Sayed, "Optimal linear cooperation for spectrum sensing in cognitive radio networks," *IEEE Journal of selected topics in signal processing*, vol. 2, no. 1, pp. 28–40, 2008.
- [6] W. Zhang, R. Mallik, and K. Letaief, "Cooperative spectrum sensing optimization in cognitive radio networks," in *Proc. IEEE International Conference on Communications (ICC)*, pp. 3411–3415, 2008.
- [7] L. Ding, T. Melodia, S. Batalama, J. Matyjas, and M. Medley, "Cross-layer routing and dynamic spectrum allocation in cognitive radio ad hoc networks," *IEEE Transactions on Vehicular Technology*, vol. 59, no. 4, pp. 1969–1979, 2010.

- [8] Y. Zhao, S. Min, and C. Xin, "A weighted cooperative spectrum sensing framework for infrastructure-based cognitive radio networks," *Computer Communications, Elsevier Computer Science*, vol. 34, pp. 1510–1517, 2011.
- [9] C. Cordeiro and K. Challapali, "C-mac: a cognitive mac protocol for multi-channel wireless networks," in *Dynamic Spectrum Access Networks (DySPAN)*, pp. 147–157, 2007.
- [10] S. Hung, Y. Cheng, E. Wu, and G. Chen, "An Opportunistic Cognitive MAC Protocol for Coexistence with WLAN," in *IEEE International Conference on Communications (ICC)*, pp. 4059–4063, 2008.
- [11] S. Jafar and S. Srinivasa, "Capacity limits of cognitive radio with distributed and dynamic spectral activity," *IEEE Journal on Selected Areas in Communications*, vol. 25, no. 3, pp. 529–537, 2007.
- [12] S. Srinivasa and S. Jafar, "Cognitive radio networks: how much spectrum sharing is optimal?," in *IEEE Global Telecommunications Conference (GLOBECOM)*, pp. 3149–3153, 2007.
- [13] D. Cabric, S. Mishra, and R. Brodersen, "Implementation issues in spectrum sensing for cognitive radios," in *Thirty-Eighth Asilomar Conference on Signals, Systems and Computers*, vol. 1, pp. 772–776, 2004.
- [14] P. Sutton, K. Nolan, and L. Doyle, "Cyclostationary signatures in practical cognitive radio applications," *IEEE Journal on Selected Areas in Communications*, vol. 26, no. 1, pp. 13–24, 2008.



- [15] V. Turunen, M. Kosunen, A. Huttunen, S. Kallioinen, P. Ikonen, A. Parssinen, and J. Ryynanen, "Implementation of cyclostationary feature detector for cognitive radios," in *IEEE Cognitive Radio Oriented Wireless Networks and Communications (CROWNCOM)*, pp. 1–4, 2009.
- [16] L. Luo, N. Neihart, S. Roy, and D. Allstot, "A two-stage sensing technique for dynamic spectrum access," *IEEE Transactions on Wireless Communications*, vol. 8, no. 6, pp. 3028–3037, 2009.
- [17] S. Fazeli-Dehkordy, K. Plataniotis, and S. Pasupathy, "Two-stage spectrum detection in cognitive radio networks," in *IEEE International Conference on Acoustics Speech and Signal Processing (ICASSP)*, pp. 3118–3121, 2010.
- [18] Y. Zeng and Y. Liang, "Eigenvalue-based spectrum sensing algorithms for cognitive radio," *IEEE Transactions on Communications*, vol. 57, no. 6, pp. 1784–1793, 2009.
- [19] Z. Tian and G. Giannakis, "A wavelet approach to wideband spectrum sensing for cognitive radios," in *International Conference on Cognitive Radio Oriented Wireless Networks and Communications*, pp. 1–5, 2006.
- [20] D. Liu, P. Ning, A. Liu, C. Wang, and W. Du, "Attack-resistant location estimation in wireless sensor networks," *ACM Transactions on Information and System Security (TISSEC)*, vol. 11, no. 4, pp. 1–39, 2008.
- [21] Y. Zhang, W. Liu, W. Lou, and Y. Fang, "Location-based compromise-tolerant security mechanisms for wireless sensor networks," *IEEE Journal on Selected Areas in Communications*, vol. 24, no. 2, pp. 247–260, 2006.

- [22] G. Ganesan and Y. Li, "Cooperative spectrum sensing in cognitive radio networks," in *Proc. IEEE International Symposium on New Frontiers in Dynamic Spectrum Access Networks (DySPAN)*, pp. 137–143, 2005.
- [23] W.-Y. Lee and I. Akyildiz, "Optimal spectrum sensing framework for cognitive radio networks," in *IEEE Transactions on Wireless Communications*, vol. 7, pp. 3845–3857, 2001.
- [24] W. Saad, Z. Han, M. Debbah, A. Hjørungnes, and T. Basar, "Coalitional games for distributed collaborative spectrum sensing in cognitive radio networks," in *Proc. IEEE INFOCOM*, pp. 2114–2122, 2009.
- [25] R. Chen, J.-M. Park, and K. Bian, "Robust distributed spectrum sensing in cognitive radio networks," in *Proc. IEEE INFOCOM*, pp. 1876–1884, 2008.
- [26] J. Lee, Y. Kim, S. Sohn, and J. Kim, "Weighted-cooperative spectrum sensing scheme using clustering in cognitive radio systems," in *Proc. ICACT*, pp. 786–790, 2008.
- [27] B. Shen, L. Huang, C. Zhao, K. Kwak, and Z. Zhou, "Weighted Cooperative Spectrum Sensing in Cognitive Radio Networks," in *Proc. Third International Conference on Convergence and Hybrid Information Technology (ICCIT)*, pp. 1074–1079, 2008.
- [28] S. Mishra, A. Sahai, and R. Brodersen, "Cooperative sensing among cognitive radios," in *Proc. IEEE International Conference on Communications (ICC)*, pp. 1658–1663, 2006.

- [29] C. Stevenson, G. Chouinard, Z. Lei, W. Hu, S. Shellhammer, and W. Caldwell, "Ieee 802.22: The first cognitive radio wireless regional area network standard," *IEEE Communications Magazine*, vol. 47, no. 1, pp. 130–138, 2009.
- [30] Q. Zhao, L. Tong, A. Swami, and Y. Chen, "Decentralized cognitive mac for opportunistic spectrum access in ad hoc networks: A pomdp framework," *IEEE Journal on Selected Areas in Communications*, vol. 25, no. 3, pp. 589–600, 2007.
- [31] Y. Bae, A. Alfa, and B. Choi, "Performance analysis of modified ieee 802.11-based cognitive radio networks," *IEEE Communications Letters*, vol. 14, no. 10, pp. 975–977, 2010.
- [32] D. Xue, E. Ekici, and X. Wang, "Opportunistic periodic mac protocol for cognitive radio networks," in *Proc. IEEE GLOBECOM*, pp. 1–6, 2010.
- [33] P. Wang, D. Niyato, and H. Jiang, "Voice-service capacity analysis for cognitive radio networks," *IEEE Transactions on Vehicular Technology*, vol. 59, no. 4, pp. 1779–1790, 2010.
- [34] S. Akin and M. Gursoy, "Performance analysis of cognitive radio systems under qos constraints and channel uncertainty," in *Proc. IEEE GLOBECOM*, pp. 1–5, 2010.
- [35] A. Attar, N. Devroye, H. Li, and V. Leung, "Achieving fairness in distributed cognitive radio networks using a timer mechanism," in *IEEE International Symposium on Wireless Communication Systems (ISWCS)*, pp. 1041–1045, 2010.

- [36] W. Ahmed, J. Gao, H. Zhou, and M. Faulkner, "Throughput and proportional fairness in cognitive radio networks," in *IEEE International Conference on Advanced Technologies for Communications (ATC)*, pp. 248–252, 2009.
- [37] O. Simeone, Y. Bar-Ness, and U. Spagnolini, "Stable throughput of cognitive radios with and without relaying capability," *IEEE Transactions on Communications*, vol. 55, no. 12, pp. 2351–2360, 2007.
- [38] F. Borgonovo, M. Cesana, and L. Fratta, "Throughput and delay bounds for cognitive transmissions," *Advances in Ad Hoc Networking*, pp. 179–190, 2008.
- [39] Y. Hou, Y. Shi, and H. Sherali, "Spectrum sharing for multi-hop networking with cognitive radios," *IEEE Journal on Selected Areas in Communications*, vol. 26, no. 1, pp. 146–155, 2008.
- [40] H. Shiang and M. van der Schaar, "Queuing-based dynamic channel selection for heterogeneous multimedia applications over cognitive radio networks," *IEEE Transactions on Multimedia*, vol. 10, no. 5, pp. 896–909, 2008.
- [41] M. Thathachar and P. Sastry, "Varieties of learning automata: an overview," *IEEE Transactions on Systems, Man, and Cybernetics, Part B: Cybernetics*, vol. 32, no. 6, pp. 711–722, 2002.
- [42] Y. Song, Y. Fang, and Y. Zhang, "Stochastic channel selection in cognitive radio networks," in *Proc. IEEE GLOBECOM*, pp. 4878–4882, 2007.

- [43] S. Shetty, M. Song, C. Xin, and E. Park, "A learning-based multiuser opportunistic spectrum access approach in unslotted primary networks," in *Proc. IEEE INFOCOM*, pp. 2966–2970, 2009.
- [44] J. Unnikrishnan and V. Veeravalli, "Cooperative sensing for primary detection in cognitive radio," in *IEEE Journal of Selected Topics in Signal Processing*, pp. 18–27, 2008.
- [45] E. Peh and Y. Liang, "Optimization for cooperative sensing in cognitive radio networks," in *Proc. IEEE Wireless Communications and Networking Conference (WCNC)*, pp. 27–32, 2007.
- [46] F. Digham, M. Alouini, and M. Simon, "On the energy detection of unknown signals over fading channels," in *Proc. IEEE International Conference on Communications (ICC)*, pp. 3575–3579, 2003.
- [47] P. V. Miegheem in *Performance Analysis of Communications Networks and Systems*, pp. 103–104, Cambridge University Press, 2006.
- [48] F. F. Digham., M.-S. Alouini., and M. K. Simon, "On the energy detection of unknown signals over fading channels," in *Proc. IEEE International Conference on Communications (ICC)*, pp. 3575–3579, 2005.
- [49] T. S. Rappaport, "Wireless communications, principles and practice, 2nd Ed," *Prentice Hall*, 2002.
- [50] "E3 white paper, spectrum sensing," Nov. 2009.

- [51] Y. Zhao, S. Min, and C. Xin, "A weighted cooperative spectrum sensing framework for infrastructure-based cognitive radio networks," *Computer Communications, Elsevier Computer Science*, vol. 34, pp. 1510–1517, 2011.
- [52] G. Bianchi, "Performance analysis of the ieee 802.11 distributed coordination function," *IEEE Journal on Selected Areas in Communications*, vol. 18, no. 3, pp. 535–547, 2000.
- [53] G. Berger-Sabbatel, A. Duda, M. Heusse, and F. Rousseau, "Short-term fairness of 802.11 networks with several hosts," *Mobile and Wireless Communication Networks*, pp. 263–274, 2005.
- [54] D. Bertsekas and R. Gallager, *Data Networks*. Prentice Hall, Jan. 1992.
- [55] C. Xin, M. Song, L. Ma, G. Hsieh, and C.-C. Shen, "On random dynamic spectrum access for cognitive radio networks," in *Proc. IEEE Globecom*, 2010.
- [56] R. Tandra and A. Sahai, "SNR walls for signal detection," *IEEE Journal of Selected Topics in Signal Processing*, vol. 2, no. 1, pp. 4–17, 2008.

## VITA

Yanxiao Zhao

Department of Electrical and Computer Engineering

Old Dominion University

Norfolk, VA 23529

### EDUCATION

**M.S.**, Electronic and Information Engineering, Xi'an Jiaotong University, China, 2005,

**B.S.**, Information and Control Engineering, Xi'an University of Architecture and Technology, China, 2001,

### SELECTED PUBLICATIONS

[1] **Y. Zhao**, M. Song, and C. Xin, "A Weighted Cooperative Spectrum Sensing Framework for Infrastructure-based Cognitive Radio Networks," *Computer Communications*, Elsevier, vol. 34, Issue 12, Pages 1510-1517, 2011.

[2] **Y. Zhao** and M. Song, "Access Point Selection Algorithm for Multi-rate WLANs to Optimise Throughput and Guarantee Fairness," *International Journal of Ad Hoc and Ubiquitous Computing*, vol. 8, no. 3, 2011.

[3] **Y. Zhao**, M. Song, C. Xin and M. Wadhwa, "Spectrum Sensing Based on Three-State Model to Accomplish All-level Fairness for Co-existing Multiple Cognitive Radio Networks", *IEEE INFOCOM 2012*, Mar 2012. (Acceptance Rate: 278/1547=18%).

[4] **Y. Zhao**, M. Song and C. Xin, "Delay Analysis for Cognitive Radio Networks Supporting Heterogeneous Traffic," *IEEE Communications Society Conference on Sensor, Mesh and Ad Hoc Communications and Networks (SECON)*, Jun 2011 (Acceptance Rate: 66/241=27%).

[5] **Y. Zhao**, M. Song, J. Wang and E. K. Park, "Throughput Measurement-based Access Point Selection for Multi-rate Wireless LANs," *International Conference on Wireless Algorithms, Systems, and Applications (WASA)*, **Best Paper Award** (2 out of 68 accepted papers), Aug 2009.

[6] M. Song, **Y. Zhao**, J. Wang and E. K. Park, "A High Throughput Load Balance Algorithm for Multichannel Wireless Sensor Networks," *IEEE International Conference on Communications (ICC)*, Jun 2009 (Acceptance Rate: 1046/3000= 34.9%).